



HAL
open science

Combined effects of ocean warming and acidification on the larval stages of the European abalone *Haliotis tuberculata*

Javid Kavousi, Sabine Roussel, Sophie Martin, Fanny Gaillard, Aicha Badou, Carole Di Poi, Sylvain Huchette, Philippe Dubois, Stéphanie Auzoux-Bordenave

► To cite this version:

Javid Kavousi, Sabine Roussel, Sophie Martin, Fanny Gaillard, Aicha Badou, et al.. Combined effects of ocean warming and acidification on the larval stages of the European abalone *Haliotis tuberculata*. *Marine Pollution Bulletin*, 2022, 175, pp.113131. 10.1016/j.marpolbul.2021.113131 . hal-03485433

HAL Id: hal-03485433

<https://hal.univ-brest.fr/hal-03485433v1>

Submitted on 22 Jul 2024

HAL is a multi-disciplinary open access archive for the deposit and dissemination of scientific research documents, whether they are published or not. The documents may come from teaching and research institutions in France or abroad, or from public or private research centers.

L'archive ouverte pluridisciplinaire **HAL**, est destinée au dépôt et à la diffusion de documents scientifiques de niveau recherche, publiés ou non, émanant des établissements d'enseignement et de recherche français ou étrangers, des laboratoires publics ou privés.



Distributed under a Creative Commons Attribution - NonCommercial 4.0 International License

1 **“Combined effects of ocean warming and acidification on the larval stages of the European**
2 **abalone *Haliotis tuberculata*”**

3 Javid Kavousi¹, Sabine Roussel¹, Sophie Martin^{2,3}, Fanny Gaillard³, Aicha Badou⁴, Carole Di
4 Poi⁵, Sylvain Huchette⁶, Philippe Dubois⁷, Stéphanie Auzoux-Bordenave^{2,8}

5 ¹Univ Brest, CNRS, IRD, Ifremer, LEMAR, Plouzane, France

6 ²Sorbonne Université, 4 place Jussieu, Paris 75005, France

7 ³UMR 7144 “Adaptation et Diversité en Milieu Marin” (AD2M), CNRS/SU, Station Biologique de
8 Roscoff, Roscoff Cedex 29680, France

9 ⁴Direction Generale Deleguee a la Recherche, l’Expertise, la Valorisation et l’Enseignement (DGD
10 REVE), Muséum National d’Histoire Naturelle, Station marine de Concarneau, Concarneau 29900,
11 France

12 ⁵Ifremer, LEMAR UMR 6539 UBO/CNRS/IRD/Ifremer, Argenton, France

13 ⁶Ecloserie France Haliotis, Kerazan, Plouguerneau 29880, France

14 ⁷Laboratoire de Biologie Marine, Université Libre de Bruxelles, CP160/15, 1050, Brussels, Belgium

15 ⁸UMR “Biologie des Organismes et Ecosystèmes Aquatiques” (BOREA), MNHN/CNRS/SU/IRD,
16 Muséum National d’Histoire Naturelle, Station Marine de Concarneau, Concarneau 29900, France

17

18

19

20

21

22

23

24

25 **Abstract**

26 This study examined the physiological responses of the larval stages of *Haliotis tuberculata*, an
27 economically important abalone, to combined temperature (17°C and 19°C) and pH (ambient pH
28 and -0.3 units, i.e., +200% increase in seawater acidity) in a full factorial experiment. Tissue
29 organogenesis, shell formation, and shell length significantly declined due to low pH. High
30 temperature significantly increased the proportion of fully shelled larvae at 24 hours post-
31 fertilization (hpf), but increased the proportion of unshelled larvae at 72 hpf. Percentage of
32 swimming larvae at 24 hpf, 72 hpf and 96 hpf significantly declined due to high temperature, but
33 not because of low pH. Larval settlement increased under high temperature, but was not affected
34 by low pH. Despite the fact that no interaction between temperature and pH was observed, the
35 results provide additional evidence on the sensitivity of abalone larvae to both low pH and high
36 temperature. This may have negative consequences for the persistence of abalone populations in
37 natural and aquaculture environments in the near future.

38

39 **Keywords:** ocean acidification, global warming, climate change, marine mollusks, abalone
40 larvae

41

42

43

44

45 **Introduction**

46 Increased CO₂ concentrations due to anthropogenic activities have led to increased oceanic CO₂
47 absorption, resulting in a phenomenon called ocean acidification (OA) that is concurrent with
48 ocean warming (OW). Current projections suggest that by the year 2100, the average sea surface
49 temperature will increase by 1°C– 3°C and the water pH will drop by 0.1 to 0.3 units (i.e., +30%
50 to +200% increases in acidity; IPCC, 2014). OA has particularly deleterious impacts on marine
51 calcifiers that produce calcium carbonate (CaCO₃) skeletons (Kroeker et al., 2013; Parker et al.,
52 2013). These minerals are experiencing unprecedented decreases in their saturation states due to
53 ongoing OA. This has a suppressive, narcotic effect and causes acidosis, which impairs many
54 physiological processes (Feely et al., 2004; Portner, 2008; Doney et al., 2009). In contrast, the
55 impacts of increased temperatures due to OW can stimulate physiological processes until they
56 reach a threshold (Pörtner, 2010; Przeslawski et al., 2011; Byrne et al., 2011).

57 The combined impacts of OA and OW have been addressed with contrasting responses, such that
58 the effects of OA and OW are either exacerbated (e.g., Di Santo 2015; D’Amario et al., 2020;
59 Zittier et al. 2018; Rodolfo-Metalpa et al., 2011) or ameliorated (e.g., Kroeker et al. 2014; Davis
60 et al., 2013; Knights et al., 2020; García et al., 2015; Jiang et al., 2018) in the presence of the
61 other stressor (). Meta-analyses have suggested that the combined impacts of OA and OW on
62 species physiology are especially devastating for the larval stages of many species (Przeslawski
63 et al., 2015; Kroeker et al., 2013), presenting a major bottleneck for population persistence under
64 changing oceanic conditions (Przeslawski et al., 2015). As a result, the responses of these early
65 stages to combined OA and OW are now being paid greater attention (Przeslawski et al., 2015).
66 Temperature and OA-related factors, such as pH, are among the paramount environmental
67 factors that dictate the survival, morphology, physiology, and behavior of marine larvae, and in

68 particular, calcifying larvae (Przeslawski et al., 2015). Among all of the marine calcifiers studied
69 so far, mollusk larvae are the most vulnerable to the effects of OA (Przeslawski et al., 2015;
70 Kroeker et al., 2013).

71 The recent marine mollusks include over 43,000 recognized species That includes some of the
72 major CaCO₃ producers (Rosenberg, 2014) fulfilling crucial ecosystem functions, such as
73 creating habitat structures and food sources for benthic species (Parker et al., 2013). Therefore,
74 any negative impacts from environmental drivers can result in high ecological and economic
75 consequences (Narita et al., 2012). Abalones are important mollusks that have high ecological
76 and commercial values, and also provide food for human beings (Cook, 2016; Huchette and
77 Clavier, 2004). However, their natural populations have experienced severe declines due to
78 overexploitation (Micheli et al., 2008; Kashiwada and Taniguchi, 2007) and environmental
79 disturbances such as OW and bacterial diseases (Cook, 2016; Travers et al., 2009; Huchette and
80 Clavier, 2004; Morales-Bojórquez et al., 2008). On the other hand, abalone aquaculture is
81 expanding worldwide, understanding the effects of global change drivers on abalone physiology
82 is an important issue for the management of abalone populations in natural and aquaculture
83 environments (Morash and Alter, 2015).

84 Early life-history stages of abalones are negatively affected by OA and show a high percentage
85 of deformed larvae under low-pH conditions (Byrne et al., 2011; Crim et al., 2011; Guo et al.,
86 2015; Kimura et al., 2011; Zippay and Hofmann, 2010; Wessel et al., 2018; Swezey et al., 2020).

87 Other negative responses that have been reported in abalones in response to temperatures higher
88 than their physiological limit during development include abnormal appearance, reduced growth,
89 and trochophore mortality (e.g., Leighton, 1974; Pedroso, 2017). Although several studies have
90 shown larval abalones to be highly sensitive to OA (Santander-De Leon et al., 2018; Crim et al.,

91 2011; Tahil and Dy, 2016; Guo et al., 2015; Wessel et al., 2018), the combined effects of OA and
92 OW are still not understood (Gao et al., 2020). Based on the limited data available, OA and OW
93 may have deleterious impacts on abalone populations. Indeed, *Haliotis coccoradiata* embryos
94 were dramatically affected by a combination of high temperatures (+2 to +4°C compared with
95 control 20°C) and acidified conditions (-0.4 to -0.6 pH units), with only a small percentage
96 surviving (Byrne et al., 2011).

97 *Haliotis tubercula* is a commercially important species in Europe, for which rearing over the
98 whole life cycle is controlled in aquaculture (Huchette and Clavier, 2004; Courtois de Viçose et
99 al., 2007). As for most marine molluscs, abalone species display a pelago-benthic life cycle with
100 a larval planktonic stage followed by a critical metamorphosis into the benthic juvenile, making
101 the specie highly sensitive to environmental changes (Byrne et al. 2011). The impacts of OA on
102 all stages of the European abalone, *Haliotis tuberculata* (Linnaeus, 1758) have been recently
103 studied (Wessel et al., 2018; Auzoux-Bordenave et al., 2020; Avignon et al., 2020). All the
104 aforementioned studies reported adverse impacts of OA on *H. tuberculata*, especially on the shell
105 growth and calcification. However, *H. tuberculata* larvae were more impaired by OA than was
106 any other life stage, showing significantly adverse effects in survival rate, morphology and
107 development, growth rate and shell calcification (Wessel et al., 2018). While the impacts of OA
108 on abalone larvae are worrying enough, high temperatures present another emerging threat for *H.*
109 *tuberculata* populations (Travers et al., 2009; Huchette and Clavier, 2004). Furthermore, there is
110 a lack of knowledge on how climate change will modify *H. tuberculata* larval settlement,
111 behaviour and physiology in early life stages.

112 In this study, we investigated the combined effects of OA and OW on the early life stages of *H.*
113 *tuberculata* in a full factorial experiment. Abalone larvae were exposed to four OA and OW

114 scenarios: ambient (pH 8.08.0 and 17°C); combined (pH 7.77.7 and 19°C); and individual effect
115 scenarios (pH 8.08.0 and 19°C; pH 7.77.7 and 17°C) throughout the five days of larval
116 development. We focused on three key larval stages: the trochophore stage, characterized by the
117 set-up of the larval shell at 24 hours post-fertilization (hpf); the mature veliger stage (72 hpf);
118 and the premetamorphic veliger stage (96 hpf), which is the last pelagic life stage before larval
119 settlement (Jardillier et al., 2008; Auzoux-Bordenave et al., 2010). To better understand both the
120 individual and combined effects of OA and OW, we investigated several biological parameters
121 involved in growth, physiology and behavior throughout the larval development cycle of *H.*
122 *tuberculata*.

123

124 **Materials and methods**

125 *Abalone larvae production*

126 The parental *H. tuberculata* stock was composed of wild broodstock (3 females and 7 males)
127 collected from Saint Quay Portrieux (Brittany, France), and farmed abalones (4 females and 5
128 males) collected from an offshore sea-cage structure at the France *Haliotis* abalone farm
129 (48°36'50 N, 4°36'3 W; Plouguerneau, Brittany, France). Mixing wild and farmed broodstocks
130 prevent inbreeding and production of enough larvae for the experiment. In France *Haliotis* farm,
131 after a 10-month period in nursery tank, abalone are placed in sea-cages and raised with similar
132 environmental conditions as the wild abalone apart the protection from the predator attacks and
133 high density until the age of 4 years. They are fed with algae collected on the shore, and
134 submitted to the same temperature and pH as the wild broodstock.

135 The wild and farmed abalones were transferred from the sea and sea cages to the farm,
136 respectively. There were given time to acclimatize to the farm's conditions over three months
137 with natural running seawater maintained at 15°C and pumped twice a day from the sea, with *ad*
138 *libitum* feeding to assure optimal reproduction maturity. Spawning was induced at the France
139 *Haliotis* farm following usual procedures. Briefly, abalones were detached from the rearing
140 aquarium and placed individually into 5-L buckets. Spawning was stimulated with ultraviolet
141 light while gradually heating the filtered seawater from 18°C to 21°C over the course of 1 h.
142 Abalones were allowed to spawn for a maximum of 5.5 h from the start of the experiment. Once
143 spawned, the eggs were pooled and then divided into 12 batches. Spermatozoa from each of the
144 12 males (one male per batch of eggs) were added separately to avoid spermatoc competition
145 (Harney et al., 2018) at an optimal sperm concentration of approximately 100,000 spermatozoa
146 per egg (Huchette et al., 2004). After 1 h, the fertilized eggs were pooled again and their density
147 was estimated under a binocular microscope. The pooled fertilized eggs were then divided into
148 12 samples of 900,000 embryos per batch and transferred to the 12 hatching boxes.

149

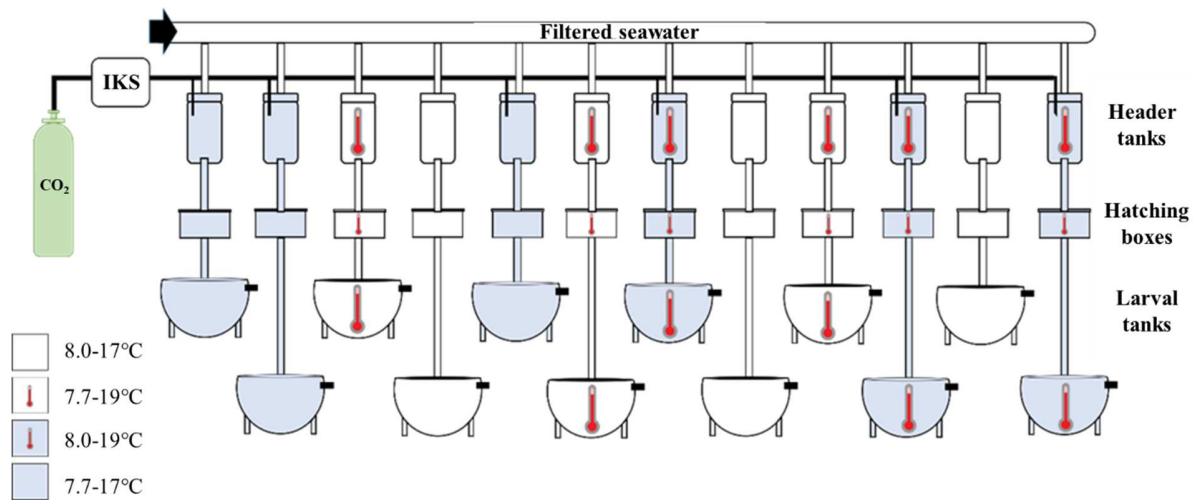
150 *Experimental design*

151 To study the individual and combined impacts of OA and OW, we applied a full factorial design
152 of two temperatures (17°C low and 19°C elevated) and two pH values (8.0 high and 7.7 low;
153 with three replicate tanks per treatment (12 tanks in total; Fig. 1). We considered 17°C to be the
154 ambient (“low”) temperature, as it was the temperature experienced by abalones during the
155 summer reproduction period in Northern Brittany. According to Gac et al. (2020), temperature in
156 the Northern Brittany reach maximal summer value of 17°C and present short-term variability of
157 0.1 to 0.4 °C mainly related to the tidal cycle and the day-time. Similarly, the high pH

158 corresponded to the naturally occurring pH during autumn in Northern Brittany (Qui-Minet et
159 al., 2018), that is, the high pH in this experiment was the ambient pH of the seawater pumped
160 into the France *Haliotis* site. The high temperature and low pH conditions were chosen based on
161 the global projections for the coming decades (IPCC, 2014). We chose the worst-case pH and
162 temperature scenarios; however, the high temperature treatment in this study is about 1°C lower
163 than the worst scenarios predicted for 2100. Abalone larvae were exposed to the experimental
164 conditions from 1 h post-fertilization until they reached the premetamorphic veliger stage. The
165 temperature was controlled using two central heating systems. For the 17°C treatment and pre-
166 heating of the 19°C treatment, we used an Aquahort Ltd Heat Pump (26 kW; THP26-3). To
167 reach 19°C, we supplemented this pump with a Charot Heat Pump (6 kW; 4911 type). Each
168 replicate was composed of three parts: I) a food-safe plastic head tank (60 L), in which water of
169 the appropriate temperature and CO₂ level was premixed and homogenized with a bubbling
170 system; II) a food-safe 22.5-L hatching box (30 cm x 50 cm x 15 cm), which was supplied with
171 reduced-flow running water from the head tank to avoid flushing the eggs out while maintaining
172 the desired pH and temperature. This box harbored the fertilized eggs to allow them to hatch
173 within the first 18 h. An evacuation pipe was connected to the rearing tank to allow automatic
174 larval transfer once the larvae could swim; this transfer was completed over four hours. III) A
175 350-L epoxy-coated larval tank, which was supplied by the head tank, to rear hatched larvae that
176 had left the hatching box. Natural 3-µm filtered seawater was allowed to run through the tanks at
177 all times (open circuit). To prevent larvae from leaving the tanks, a 40-µm net was placed at the
178 outflow. The flow rate from the head tanks to the rearing tanks was between 200–400 mL·min⁻¹.
179 All tanks were exposed to an artificial photoperiod of 12 h light:12 h dark, which was provided
180 at a light intensity of 900–1000 lux at the water surface using 68-W natural spectrum light-

181 emitting diode (LED) lamps (Solar Natur, JBL). As pre-settlement abalone larvae are
182 lecithotrophic (non-feeding), they were not fed during the experiment.

183



184

185 **Fig. 1** Simplified design of the experimental system showing the flow of filtered seawater from
186 the header tanks, the styrene hatching boxes, and the 350-L larval tanks (12 in total). Seawater
187 exited the system via the black outflow at the top of larval tanks. IKS is a pH-regulated
188 electrovalve system. The four treatments are indicated using two colors (white and blue) and a
189 red thermometer for high temperatures.

190

191 *Carbonate chemistry and pH control*

192 Carbonate chemistry and pH control were monitored according to the methods of Avignon et al.
193 (2020). Low-pH seawater was provided by bubbling CO₂ (Air Liquide, Paris, France) into the
194 tanks through electrovalves regulated by a pH-stat system (Aquastar, IKS Computer System,
195 Karlsbad, Germany) (one electrovalve and bubbling CO₂ system per header tank). The desired
196 low-pH value was adjusted to be 0.3 units lower than the high pH, corresponding to natural pH

197 fluctuations along the Northern Brittany coast (the total scale (pH_T) range of 7.9–8.2; Qui-Minet
198 et al., 2018). The values of the pH-stat system were adjusted from daily measurements of the
199 electromotive force in the header tanks using a pH meter (Metrohm 826 pH mobile, Metrohm
200 AG, Herisau, Switzerland) with a glass electrode (Metrohm Ecotrode Plus, Metrohm AG,
201 Herisau, Switzerland). The electromotive force values were converted to pH units on the pH_T
202 after calibration with Tris-HCl and 2-aminopyridine-HCl (AMP) buffers (Dickson et al., 2007).

203 Temperature and salinity were measured daily using a portable conductivity meter (ProfiLine
204 Cond 3110, WTW, Oberbayern, Germany). Total alkalinity (A_T) was measured twice ($n = 12$
205 and $n = 9$) from 50-mL samples taken from each experimental tank. Seawater samples were
206 filtered through 0.7- μm Whatman GF/F membranes, immediately poisoned with mercury
207 chloride, and stored in a dark place at room temperature for later analysis.

208 A_T was determined from approximately 50 g of weighed samples using a potentiometric titration
209 at 25°C with 0.1 M HCl and using a Titrino 847 plus Metrohm. The balance point was
210 determined by the Gran method (Gran, 1952) according to Haraldsson et al. (1997). The
211 accuracy of this method was $\pm 2 \mu\text{mol}\cdot\text{kg}^{-1}$ and was verified by Certified Reference Material
212 182, provided by A. Dickson (Scripps Institute of Oceanography, University of South California,
213 San Diego, United States). The seawater carbonate chemistry analysis included dissolved
214 carbonate (CO_3^{2-}), bicarbonate (HCO_3^-), dissolved inorganic carbon (DIC), pCO_2 , aragonite
215 saturation state (Ω_{ar}), and calcite saturation state (Ω_{calc}); these were determined by entering the
216 values of pH_T , A_T , temperature, and salinity into CO2SYS software (Lewis and Wallace, 1998)
217 using constants from Mehrbach et al. (1973) as refitted by Dickson and Millerro (1987).

218

219

220

221 *Hatching success*

222 Under pH 8.0 and 17°C, trochophore larvae typically hatch at 18–20 hpf (Jardillier et al., 2008).

223 To estimate the percentage of larvae that hatched in the 12 experimental hatching boxes, we

224 collected all of the unhatched larvae that were deposited at the bottom of the hatching boxes at

225 24 hpf, after the hatched larvae could swim and had evacuated to the 350-L rearing tank. Nine 1-

226 mL replicates were sampled from a 5-L bucket and fixed with 90% ethanol. Then, the total

227 number of unhatched larvae per tank was counted under a binocular microscope. To estimate the

228 percent hatching success of each tank, we used formula 1.

229
$$(1) = \frac{\text{number of swimming larvae at 24 hpf}}{(\text{number of swimming larvae at 24 hpf} + \text{number of unhatched larvae})} \times 100$$

230

231 *Morphometric assessment and percentage of swimming larvae*

232 The post-embryonic developmental stages of *H. tuberculata* were explained in detail by Jardillier

233 et al. (2008) and Auzoux-Bordenave et al. (2010). Our morphometric measurements were

234 focused at 24 and 72 hpf, which corresponded to the free-swimming trochophore and mature

235 veliger stages, respectively. Therefore, only the swimming larvae in the tank water column that

236 corresponded to these larval stages were sampled for further analyses.

237 The development timing of the larvae was investigated under a binocular microscope at 24, 72,

238 and 96 hpf to verify the larval stages before sampling according to Jardillier et al. (2008) and

239 Auzoux-Bordenave et al. (2010). At 24 and 72 hpf, the total number of larvae swimming in each

240 tank was estimated from six 10-mL replicates per tank (n = 18 per treatment). For morphometric,
241 birefringence, and scanning electron microscopy (SEM) analysis, 10–15 L of seawater
242 containing larvae was collected from each tank and filtered through a 40- μ m sieve, then
243 aliquoted into 15-mL tubes. Larvae were concentrated at the bottom of each sample by adding
244 few drops of 70% ethanol; then, the samples were fixed and stored in 70% ethanol for polarized
245 light microscopy and SEM analysis. At 96 hpf, all of the swimming larvae were filtered out of
246 the 350-L tank using a 40- μ m sieve and placed into buckets containing 5 L of seawater adjusted
247 to the same temperature and pH as in their respective treatments. The percentage of swimming
248 larvae at 96 hpf was calculated from eight 1-mL samples (n = 24 per treatment). The percentage
249 of swimming larvae was calculated at 24 hpf, 72 hpf and 96 hpf as the total number of swimming
250 larvae in the 350-L tank at each time point divided by the initial number of larvae that hatched.

251 *Slide preparation for morphometric and birefringence analysis*

252 To study morphometric characteristics and birefringence, 12 slides per larval stage (1 replicate
253 per experimental tank) were prepared with the ethanol-fixed larvae (Wessel et al., 2018).
254 Approximately 100 larvae were whole-mounted in about 500 μ L of glycerol. All ethanol was
255 removed before the samples were transferred into the glycerol. The slides were kept at room
256 temperature for 5 to 10 min to allow any remaining ethanol to evaporate and let the larvae settle.
257 Six spots of vacuum gel were deposited at the corners and middle edges of a square coverslip to
258 prevent the larvae from being crushed. After placing the coverslip over the glycerol, the slides
259 were gently sealed with clear nail polish. Each slide contained 150 larvae per treatment per larval
260 stage. The first 50 larvae that were observed per slide, regardless of their orientation, shape, and
261 development, were photographed for morphological analysis with an Olympus binocular
262 microscope (Olympus, Hamburg, Germany) under phase contrast and under polarized light. The

263 same microscope was equipped with polarizing filters for the birefringence analysis. To avoid
 264 bias, a coding system was used to prevent the person taking pictures and analyzing the photos
 265 from learning which slides corresponded to the particular treatments. All images were taken with
 266 a digital camera (DS-Ri1, Nikon) at 20X magnification and a 40-ms exposure. Images were
 267 analyzed in ImageJ software (1.52a).

268

269 *Morphometric analysis*

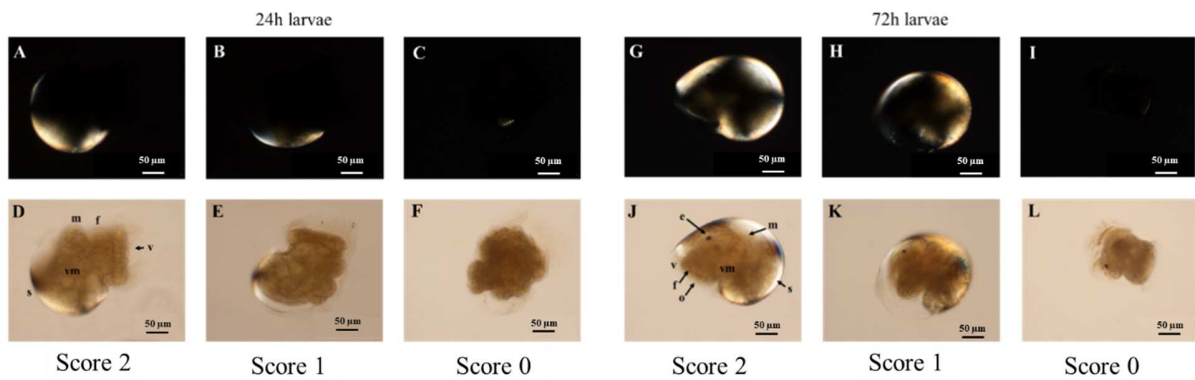
270 Larval development, shell formation, and shell size were analyzed for larvae lying on the lateral
 271 side (n = 125–133 larvae per treatment). We used semi-quantitative categorizations to analyze
 272 larval development, whereby each larva was scored on a scale from 0 to 2 as one of three
 273 morphological categories (Table 1; Fig. 2).

274

275 **Table 1** Semi-quantitative morphological categories of abalone larvae at 24 and 72 hpf.
 276 Categories were based on shell formation and soft tissue morphogenesis according to the
 277 developmental cycle of *Haliotis tuberculata* at $17 \pm 0.5^\circ\text{C}$ (Jardillier et al. 2008).

Score	Shell formation	Soft tissue morphogenesis
2	Normal shell	Tissues normally developed
1	Shell partially and/or abnormally developed	Abnormal or partially developed
0	No shell	Undeveloped

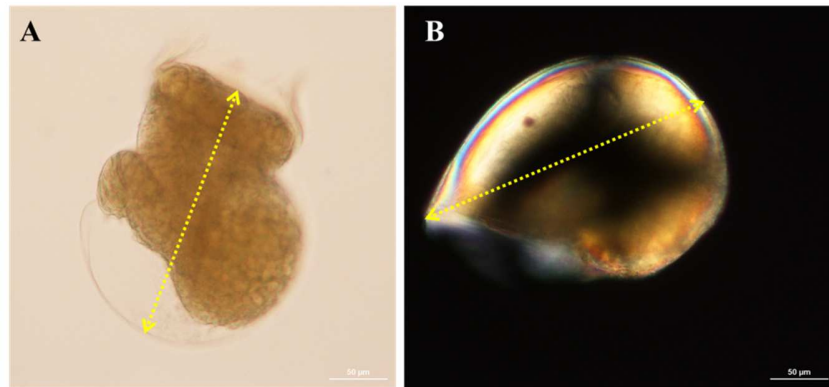
278



280

281 **Fig. 2** Polarized microscope (A–C and G–I) and light microscope (D–F and J–L) images
 282 showing the morphological variables used for larval scoring at 24 hours post-fertilization (hpf;
 283 left) and 72 hpf (right). **A** and **G** Larvae with normal shell development (score = 2; the shell field
 284 covers the posterior area of the larval body, including the light half-circled area). **B** and **H**
 285 Partially and/or abnormally developed shell (score = 1). **C** and **I** Larvae with no shell
 286 development (score = 0). **D** Larvae at 24 hpf with normal tissue development (score = 2). **J**
 287 Larvae at 72 hpf with normal tissue development (score = 2) . **E** and **K** Partially and/or
 288 abnormally developed larvae (score = 1). **F** and **L** Underdeveloped larvae (score = 0). velum (v),
 289 mantle (m), shell (s), foot (f), visceral mass (vm), eyes (e), and operculum (o)

290 The maximum larval length (24 hpf) or total shell length (72 hpf) were measured using ImageJ
 291 software and used as indicators of larval size, with all individuals lying on the lateral side (Fig.
 292 3). The mean length of larvae from each tank was calculated, and the average value for all tank
 293 replicates was presented as the mean larva size for each treatment (n = 3 tanks per treatment).



294

295 **Fig. 3** Larval length measured at **A** 24 hours post-fertilization (hpf) and **B** 72 hpf. Arrow heads
296 show the two ends of the measured lengths. Scales are 50 µm.

297 *Birefringence analysis*

298 We measured birefringence on a scale of 0–255 under cross-polarized light using an Olympus
299 microscope, according to the method described by Wessel et al. (2018). Cross-polarized light
300 that passes through CaCO₃ (an anisotropic material) is double-refracted, and shells with higher
301 CaCO₃ content double-refract more light. Therefore, birefringence intensity can be used as a
302 proxy for evaluating shell mineralization (Noisette et al., 2014). Birefringence was measured for
303 at least 120 larvae per treatment at 24 and 72 hpf using ImageJ. The mean grayscale level (in
304 pixels) was determined for each area of the larval shell showing birefringence, i.e., two zones for
305 24 hpf larvae, and three zones for 72 hpf larvae.

306

307 *Scanning electron microscopy*

308 Larvae stored in 70% ethanol were used for SEM analysis (four larvae per treatment). Samples
309 were dehydrated in a series of increasingly concentrated ethanol solutions (90%, 95%, and
310 100%) and were critical point dried with liquid CO₂. Finally, the samples attached to the SEM

311 stubs were gold-coated and observed at 5 kV with a SIGMA 300 FE-SEM scanning electron
312 microscope (Plateau Technique de Microscopie Electronique, MNHN, Concarneau, France).

313

314 *Larval swimming behavior*

315 At 72 hpf, a 1-L sample was taken from each 350-L tank by carefully dipping a plastic bucket
316 into the middle of the tank and filling it to its maximum capacity. The bucket was covered with a
317 lid to minimize CO₂ exchange and ensure pH stability. The samples were kept in insulated boxes
318 to maintain their respective temperature treatments while they were transported (< 45 min) to the
319 Institut Français de Recherche pour l'Exploitation de la Mer (IFREMER) experiment station
320 (Argenton, France). Upon arrival, the buckets were placed in water baths adjusted to their
321 respective treatment temperatures to recover from their transport. After two hours, the samples
322 were examined for the behavioral analysis.

323 The pH treatments were randomly selected for behavioral analysis, alternating the elevated and
324 low temperatures. Before filtration, each bucket's temperature and pH were measured to ensure
325 that the treatment conditions had been maintained. Larvae were concentrated in a 40- μ m sieve
326 and collected with a pipette. A total of 10–20 larvae per sample were distributed into 24-well
327 plates. The wells (16 mm in diameter) were filled with 500 μ L of natural seawater with the same
328 temperature and pH as in their original treatment (n = 3 or 4 replicates per tank). All larvae were
329 allowed to habituate for 5 min prior to starting the test. Videos were recorded in the DanioVision
330 Observation Chamber[®] (Noldus Information Technology, the Netherlands) using a camera
331 (Basler, GigE) fitted with a 55-mm lens that was positioned 15 cm away from the microplate.
332 Each video was recorded for 30 seconds at 30 frames per second and 1920 \times 1080 resolution. All

333 processed videos were analyzed under completely treatment-blind conditions using the software
334 EthoVision XT 13.0 (Noldus Information Technology, Wageningen, the Netherlands). This
335 software tracked active larval swimming for a maximum of 16 larvae simultaneously (not
336 exceeded in our case) within a selected area. To reduce uncertainty, we pre-set a few criteria that
337 were followed for each video. For example, if the larvae hit the walls of the well or if they
338 collided, the behavioral variables after the collision were excluded from further analysis.
339 Therefore, only larvae that were detected for at least 10 consecutive seconds without interruption
340 were used in our analyses. If a larva did not move for 30 consecutive seconds, then no signal was
341 detected by the program and a value of zero was indicated for the different behavioral variables
342 of that larva.

343

344 The 2D_distance moved was measured as the distance (cm) that each larva traveled from the
345 center point of the well over 30 sec. The mean velocity ($\text{cm}\cdot\text{ms}^{-1}$) was calculated by dividing the
346 distance moved by the unit of time (ms). The mean meander ($\text{deg}\cdot\text{cm}^{-1}$) was calculated as the
347 mean change in a larva's direction of movement relative to its distance moved; this provided an
348 indication of how convoluted the larva's trajectory was.

349 *Larval metabolism*

350 At 72 hpf, larval respiration rates were determined using closed incubations in acrylic
351 respirometry chambers (Engineering and Design Plastics Ltd, Cambridge, UK). We carried out
352 six incubations for each experimental tank: three incubations with larvae in 120-mL respirometry
353 chambers, and three incubations with larvae-excluded seawater (control) in 80-mL respirometry
354 chambers. We applied a correction to compensate for the differences in chamber volume. About

355 100 L of live larvae were siphoned from the experimental tanks and resuspended in 1 L of
356 filtered seawater from the experimental tanks to reach a density of 100 larvae·mL⁻¹. The
357 incubation chambers that contained larvae were filled with this same larval resuspension,
358 whereas the control chambers were filled with filtered seawater from the experimental tanks. The
359 chamber temperatures were maintained at the larval culture temperature during the incubations,
360 either at room temperature (17°C) or at an high temperature (19°C) using a circulating water
361 bath. The respiration rates were calculated from the measured differences in oxygen
362 concentration during each incubation using a noninvasive fiber-optical system (FIBOX 3,
363 PreSens, Regensburg, Germany) made up of an optical fiber and a reactive oxygen spot attached
364 to the inner wall of each chamber. The reactive oxygen spots were calibrated using a 0% oxygen
365 buffer that was prepared by dissolving 10 g of Na₂SO₃ into 1 L of seawater, and a 100% oxygen
366 buffer that was prepared by bubbling air into 1 L of seawater for 20 min to achieve oxygen
367 saturation. Oxygen consumption was measured over 1.5 to 2 hours and checked for linearity.
368 Respiration rates were corrected for oxygen consumption in the controls and normalized to the
369 number of larvae ($\mu\text{mol O}_2\cdot\text{larva}^{-1}\cdot\text{h}^{-1}$).

370 After each incubation (n = 9 per treatment), the exact number of larvae per chamber was
371 determined from six 100- μL sample replicates per chamber that were distributed into a six-well
372 plate.

373 For two of the three replicate incubations per experimental tank (n = 6 per treatment), the larvae
374 were removed from the chambers, rinsed with distilled water to remove salt, and filtered through
375 a pre-weighed Whatman GF/F 0.7- μm membrane. Filters containing larvae were dried in an oven
376 at 60°C for 48 h to determine their DW. The relative CaCO₃ content (%) was calculated from the
377 ash weight after burning at 550°C for 5 h and the DW of each sample ($\text{g CaCO}_3\cdot\text{g}^{-1}$ DW larvae).

378 *Larval settlement*

379 Larval settlement, which involves attachment to the substrate to achieve metamorphosis, occurs
380 about 4 days after fertilization in *H. tuberculata* at $17 \pm 0.5^\circ\text{C}$ (Jardillier et al., 2008). Therefore,
381 the larval settlement rate (%) was evaluated using premetamorphic 96 hpf veliger larvae.
382 Twenty-four glass aquaria (20 cm W \times 35 cm L \times 20 cm H) were filled with 12 L of seawater at
383 the same temperature and pH as in the original tanks. Temperatures were maintained by using a
384 water bath set at 19°C for half of the aquaria. The other 12 aquaria were left at the low
385 temperature of 17°C . We used a closed system with no water renewal to prevent the larvae from
386 escaping from the small aquaria. Therefore, the pH of the acidified treatment could not be
387 adjusted during the 24-h settlement period. As a result, the pH_T increased from 7.69 ± 0.04 at the
388 beginning of the test to 7.86 ± 0.03 at the end of the test. In each aquarium, we installed two 10
389 cm \times 15 cm vertical polycarbonate plates, one covered with the green microalga *Ulvelia lens*,
390 and one without *U. lens*. *Ulvelia lens* is one of the major inductive cues for the settlement of
391 abalone larvae (De Viçose et al., 2010, 2012; Daume et al., 2004), and the absence of such cues
392 can substantially reduce larval settlement rates (Searcy-Bernal et al., 1992; Slattery, 1992;
393 Daume et al., 1999). After estimating the density of the larvae, a 1-mL volume was distributed
394 using a pipette into two aquarium pseudo-replicates ($n = 6$ per treatment). The volume was
395 adjusted to create a similar density of the larvae in each aquarium. After about 24 h, we used a
396 binocular microscope to record the number of larvae that had settled on each plate. The water in
397 each tank was filtered using a $40\text{-}\mu\text{m}$ filter to collect any larvae that were unsettled or that had
398 attached to the sides and bottom of the tank. We applied low-pressure seawater to remove any
399 larvae that had attached to the tank. The larvae that were collected from each tank were
400 preserved in 70% ethanol for later counting. Finally, we calculated the percentage of settled

401 larvae per plate type (blank and *Ulvela*-covered) per treatment using the average of the two
402 pseudo-replicates per tank (formula 3).

403

$$404 \quad (3) = \frac{\text{number of settled larvae}}{\text{total larvae}} \times 100$$

405 One tank was lost for the pH-elevated and 17°C treatment, resulting in 2 instead of 3 replicates
406 for that treatment.

407

408 *Statistical analyses*

409 All statistical analyses were performed in R (version 4.0.5) and RStudio software (RStudio,
410 Boston, United States). Differences in hatching success, percentage of swimming larvae, shell
411 length, behavioral parameters, larval respiration rate, and larval settlement on *Ulvela*-covered
412 plates were assessed using a two-way analysis of variance (ANOVA) with pH, temperature, and
413 the interaction between pH and temperature as fixed factors. For all of the aforementioned
414 parameters, for each sampling time, the data were averaged per tank (n = 12 in total).
415 Subsequently, our replicates are tanks (not individual larvae). The normality of the residuals was
416 verified with a Shapiro–Wilk’s test, and the homogeneity of variances was tested using Levene’s
417 test. To study the effects of pH and temperature on the settlement rate on blank plates, we
418 applied a Wilcoxon rank sum test with continuity correction due to the presence of many zero
419 values, and because the normality of the residuals could not be verified. To study the interaction
420 between pH and temperature, we used a four-treatment-level Kruskal-Wallis rank sum test
421 followed by a post hoc Wilcoxon rank sum test with continuity correction. The p and F values of
422 two-way ANOVA are presented in the results, unless otherwise indicated.

423 To assess the frequency of the morphological and developmental parameters, we performed a
424 four-treatment-level (low pH - low temperature; low pH - high temperature; high pH - low
425 temperature; high pH - high temperature) chi-squared (χ^2) test to evaluate the effects of pH and
426 temperature on larval phenotypes at 24 and 72 hpf.

427

428

429 **Results**

430 *Carbonate chemistry and physicochemical characteristics of seawater*

431 The mean seawater temperature, salinity, and carbonate chemistry parameters are presented in
432 Table 2. The salinity was 35.18 ± 0.04 psu in all experimental tanks, and remained stable over
433 the course of the experiment. A_T measured in the experimental tanks was 2364 ± 17 $\mu\text{Eq}\cdot\text{kg}^{-1}$ and
434 remained stable over the course of the experiment and between experimental aquaria. The mean
435 pH_T values were 7.95 ± 0.04 and 7.68 ± 0.12 for the high and low-pH treatments, respectively.
436 The average temperatures were $17.40 \pm 0.55^\circ\text{C}$ and $19.35 \pm 0.53^\circ\text{C}$ for the low and high
437 temperature treatments, respectively (means \pm SD).

438

439 **Table 2** Mean parameters of seawater carbonate chemistry during the experiment. Total-scale seawater
440 pH (pH_T), temperature, salinity, and total alkalinity (A_T) were used to calculate the partial pressure of CO_2
441 (pCO_2 ; μatm), dissolved inorganic carbon (DIC; $\mu\text{mol}\cdot\text{kg}^{-1}$ SW), HCO_3^- , CO_3^{2-} , aragonite saturation state
442 (Ω_{ar}), and calcite saturation state (Ω_{calc}) using CO2SYS software. The pH_T and temperature values
443 shown represent the average value for each treatment, measured daily over the 5 days of the experiment
444 ($n = 15$ per treatment). Salinity was measured once a day over the 5 days of the experiment ($n = 5$ per
445 treatment). Results are expressed as mean \pm SD.

446

Treatment name	Treatment (pH-T°C)	Temperature (°C)	pH _r	pCO ₂ (µatm)	DIC	HCO ₃ ⁻ (µmol·kg ⁻¹) ¹⁾	CO ₃ ²⁻ (µmol·kg ⁻¹)	Ω _{ar}	Ω _{calc}
High pH – low temperature	8.0–17°C	17.5 ± 0.6	7.99 ± 0.04	478 ± 49	2122 ± 16	1950 ± 24	156 ± 10	2.40 ± 0.15	3.72 ± 0.23
Low pH – high temperature	7.7–19°C	19.4 ± 0.6	7.66 ± 0.12	1161 ± 319	2245 ± 45	2118 ± 58	88 ± 24	1.36 ± 0.37	2.10 ± 0.56
High pH – high temperature	8.0–19°C	19.3 ± 0.5	7.91 ± 0.05	593 ± 74	2147 ± 23	1985 ± 35	142 ± 14	2.20 ± 0.22	3.39 ± 0.34
Low pH – low temperature	7.7–17°C	17.3 ± 0.5	7.71 ± 0.11	999 ± 263	2236 ± 39	2109 ± 51	91 ± 21	1.40 ± 0.32	2.173 ± 0.49

447

448 *Hatching success*

449 The larval hatching success did not differ by temperature, pH, or the interaction of the two (p >
450 0.05; Table S1).

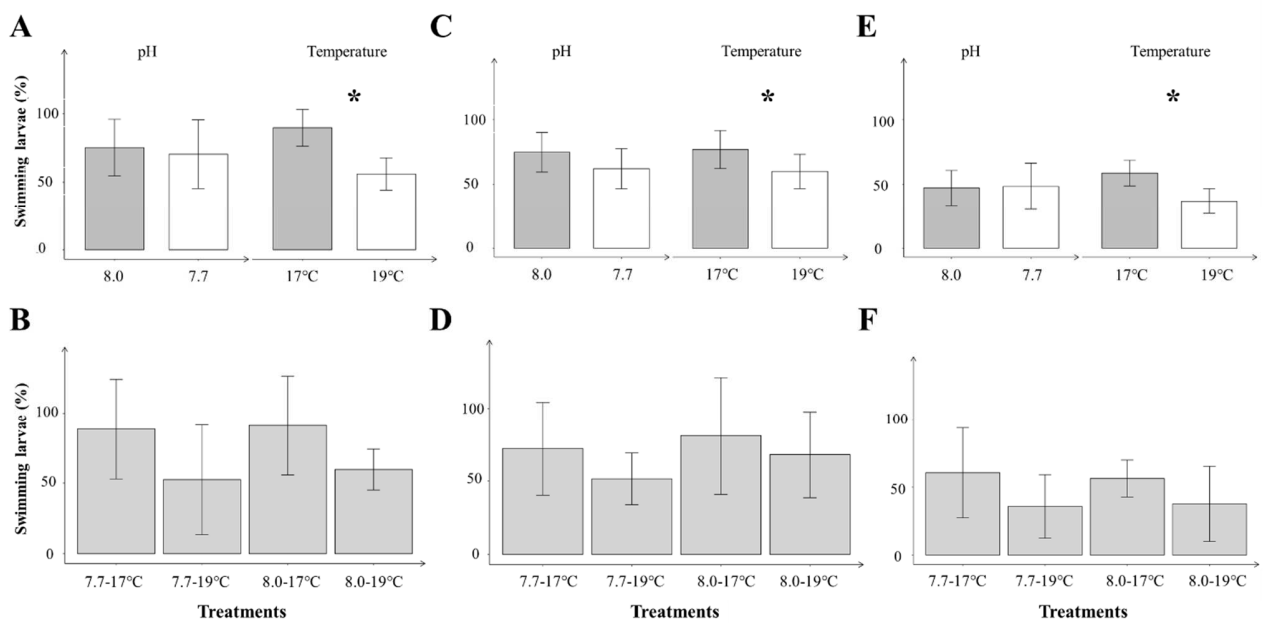
451

452

453 *Percentage of swimming larvae*

454 At 24 hpf, 72 hpf and 96 hpf the percentage of swimming larvaewas significantly lower at 19°C
 455 than at 17°C (24h hpf : $F_{1,8} = 19.92$, $p = 0.002$, Fig. 4A; 72 hpf : $F_{1,8} = 5.52$, $p = 0.046$, Fig. 4C;
 456 96 hpf : $F_{1,8} = 13.47$, $p = 0.006$, Fig. 4E). However, no pH effect (24h hpf : $F_{1,8} = 0.41$, $p =$
 457 0.539 , Fig. 4A;72 hpf : $F_{1,8} = 3.11$, $p = 0.115$, Fig. 4C; 96 hpf : $F_{1,8} = 0.04$, $p = 0.845$, Fig. 4E)
 458 and no interaction between temperature and pH (24h hpf : $F_{1,8} = 0.09$, $p = 0.764$, Fig. 4B; 72 hpf
 459 : $F_{1,8} = 0.29$, $p = 0.602$; Fig. 4D; 96 hpf : $F_{1,8} = 0.3$, $p = 0.618$; Fig. 4F) were found.

460



461

462 **Fig. 4** Effects of pH and temperature on *Haliotis tuberculata* percentage of swimming larvae at

463 **A)** 24 hours post-fertilization (hpf), **C)** 72 hpf, and **E)** 96 hpf (n = 6 tanks per treatment).

464 Combined treatment effects of pH and temperature on *H. tuberculata* percent swimming larvae

465 at **B)** 24 hpf, **D)** 72 hpf, and **F)** 96 hpf (n = 3 tanks per treatment). bar values represent means

466 and error bars represent the standard deviation of the mean. Asterisks denote significant

467 differences between temperature treatments by two-way ANOVA.

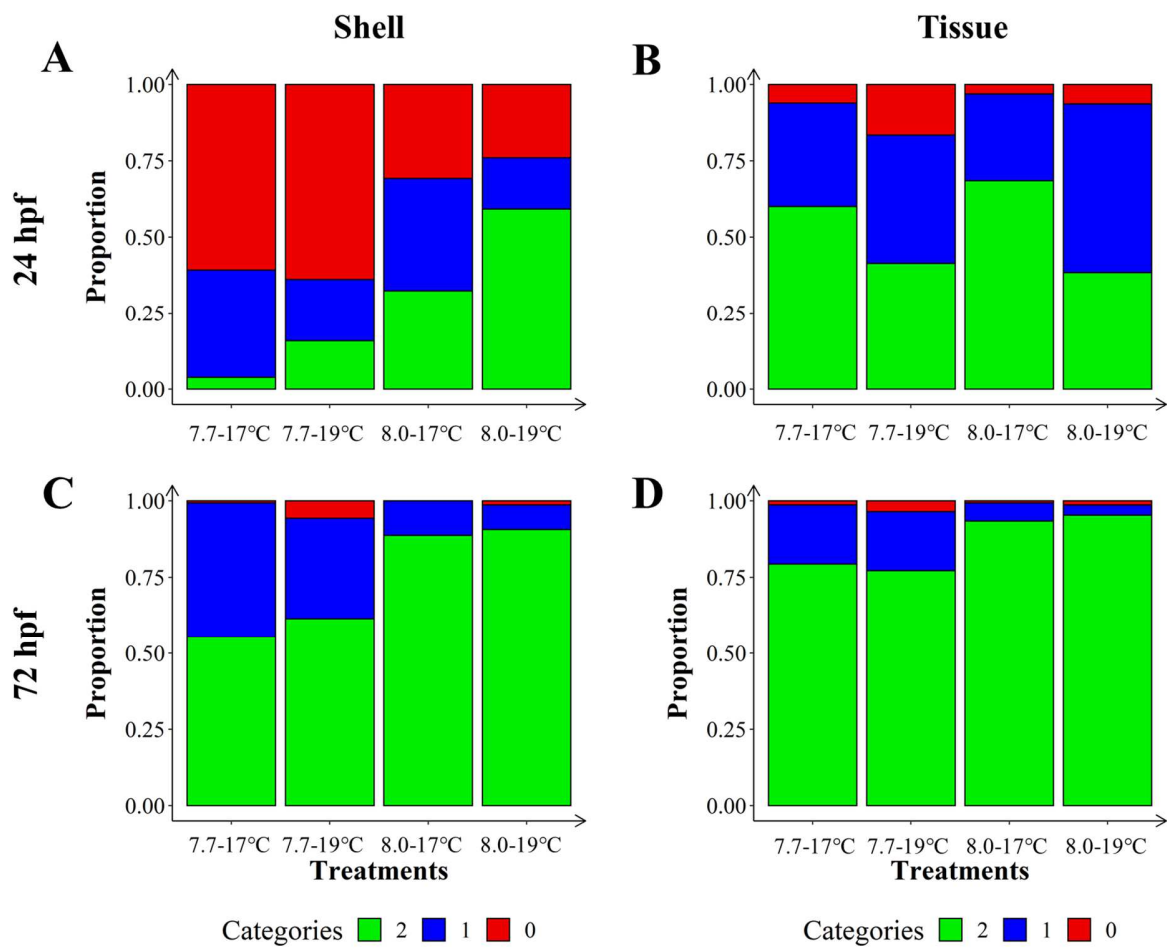
468

469

470 *Morphometric characteristics*

471 24 hpf larvae: Shell formation was significantly affected by temperature ($X^2(2) = 54.59$, $p <$
472 0.001), pH ($X^2(2) = 94.82$, $p < 0.001$), and the four treatment levels (low pH - low temperature,
473 low pH - high temperature, high pH - low temperature, high pH - high temperature); $X^2(6) =$
474 130.71 , $p < 0.001$) (Fig. 5A; Table S2). Larvae exposed to pH 7.7 were 4.5 times less likely to
475 have normal shell formation compared with larvae exposed to pH 8.0 (9.9% at pH 7.7 versus
476 45% at pH 8.0; Table S2). Larvae exposed to 19°C temperatures were 3 times as likely to have
477 normal shell formation compared with larvae exposed to 17°C temperatures (45% at 19°C versus
478 15% at 17°C; Table S2). The larvae exposed to the low pH and low temperature treatment had
479 the lowest proportion of normal shell formation, whereas larvae exposed to the high pH and high
480 temperature treatment had the highest proportion of normal shell formation (4% vs 59%,
481 respectively) (Fig. 5A; Table S2).

482 Similarly, tissue organogenesis at 24 hpf was significantly affected by temperature ($X^2(2) =$
483 24.75 , $p < 0.001$), pH ($X^2(2) = 7.83$, $p = 0.020$), and the four treatment levels (low pH - low
484 temperature, low pH - high temperature, high pH - low temperature, high pH - high temperature;
485 ($X^2(6) = 45.46$, $p < 0.001$) (Fig. 5B; Table S2). Larvae exposed to the high temperature had a
486 lower proportion of normally developed tissues than did larvae exposed to the low temperature
487 (39% at 19°C versus 61% at 17°C; Table S2), whereas larvae exposed to both low-pH and high
488 pH conditions had similar tissue organogenesis (51% at pH 7.7 versus 54% pH 8.0).



489

490 **Fig. 5** Proportional distribution of larvae at 24 hours post-fertilization (hpf) (A and B) and at 72
 491 hpf (C and D) according to their morphological categories. Colored bars indicate the degree of
 492 malformation for each variable. A and C: shell formation score (2 = normal shell; 1 = partially
 493 and/or abnormally developed shell; 0 = no shell). B and D: tissue organogenesis score (2 =
 494 normally developed tissues; 1 = partially or abnormally developed tissues; 0 = undeveloped
 495 tissues). The frequencies of each category are shown (n = 518 larvae in total).

496

497 72h larvae: Shell formation was significantly affected by temperature ($X^2(2) = 10.61$, $p =$
 498 0.005), pH ($X^2(2) = 71.19$, $p < 0.001$), and the four treatment levels (low pH - low temperature,

499 low pH - high temperature, high pH - low temperature, high pH - high temperature; $X^2 (6) =$
500 84.76, $p < 0.001$) (Fig. 5C; Table S2). Larvae exposed to pH 7.7 had a significantly lower
501 proportion of specimens with normal shell development compared with larvae exposed to the
502 high pH of 7.9 (60% at pH 7.7 versus 90% at pH 8.0) (Fig. 5C; Table S2). The larvae in the high
503 pH and high temperature treatment showed the highest proportion of specimens with normal
504 shell development (92%), followed by those in the high pH and low temperature treatment
505 (88%). Larvae exposed to the low-pH and low temperature treatment had the lowest proportion
506 of specimens with normal shell development (56%; Fig. 5C; Table S2).

507 Tissue organogenesis at 72 hpf was significantly affected by pH ($X^2 (2) = 36.15$, $p < 0.001$) and
508 by the four treatment levels (low pH - low temperature, low pH - high temperature, high pH -
509 low temperature, high pH - high temperature; $X^2 (6) = 39.54$, $p < 0.001$) (Fig. 5D; Table S1), but
510 was not significantly affected by temperature ($X^2 (2) = 2.70$, $p = 0.26$). Larvae exposed to the
511 low-pH had a significantly lower proportion of specimens with normally developed tissues
512 (78%) compared with larvae exposed to the high pH (95%; Table S2).

513

514 *Shell length*

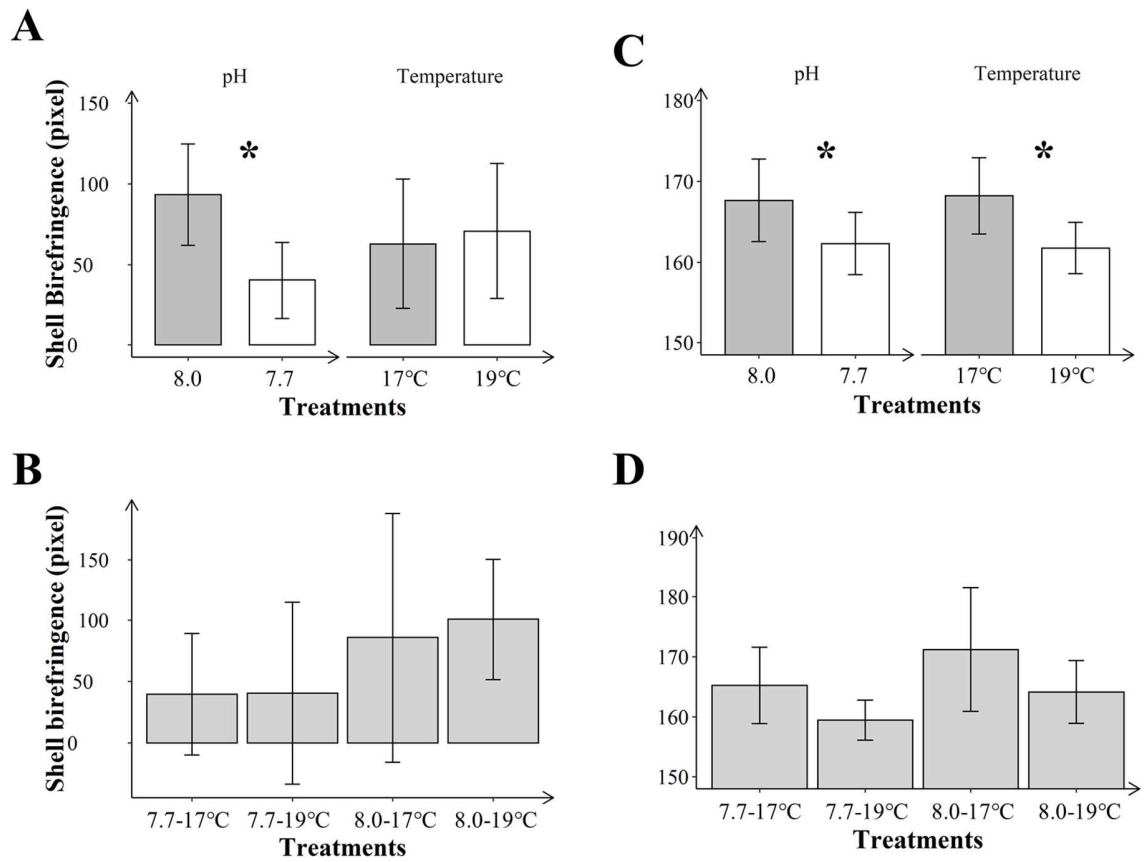
515 The shell length of the 24-hpf larvae could not be measured in the low-pH treatments because
516 there were very few larvae with normally developed shells (Fig. 5A). The shell length of the 72-
517 hpf larvae was significantly shorter in the low-pH treatments compared with the high pH
518 treatments ($F_{1,8} = 11.90$, $p = 0.008$; pH 8.0_{mean} = 265.01 ± 6.69 μm; pH 7.7_{mean} = 258.57 ± 10.61
519 μm). However, the temperature had no effect on larval shell length at 72 hpf ($F_{1,8} = 4.66$, $p =$
520 0.063; 17°C_{mean} = 264.83 ± 8.49 μm; 19°C_{mean} = 260.28 ± 8.89 μm). No interaction between

521 temperature and pH was observed ($F_{1,8} = 1.60$, $p = 0.24$; $8.0\text{--}17^\circ\text{C}_{\text{mean}} = 265.92 \pm 6.92 \mu\text{m}$; 8.0--
522 $19^\circ\text{C}_{\text{mean}} = 264.09 \pm 6.34 \mu\text{m}$; $7.7\text{--}17^\circ\text{C}_{\text{mean}} = 263.00 \pm 10.38 \mu\text{m}$; $7.7\text{--}19^\circ\text{C}_{\text{mean}} = 254.44 \pm 9.09$
523 μm).

524

525 *Shell calcification*

526 The mean birefringence (number of grayscale pixels) at 24 hpf was significantly lower at pH 7.7
527 than at the high pH of 7.9 ($F_{1,8} = 8.55$, $p = 0.019$; Fig. 6A). However, birefringence (and
528 correspondingly, shell calcification) did not differ significantly by temperature ($F_{1,8} = 1.33$, $p =$
529 0.281 ; Fig. 6A) or by the interaction between temperature and pH ($F_{1,8} = 0.01$, $p = 0.920$; Fig.
530 6B). The mean birefringence at 72 hpf was significantly lower in the pH 7.7 compared with pH
531 8.0 ($F_{1,8} = 12.21$, $p = 0.008$) and 19°C compared with 17°C ($F_{1,8} = 17.83$, $p = 0.003$) treatments,
532 indicating reduced shell calcification in low pH treatment and high temperature treatment
533 compared with the ambient pH and temperature respectively (Fig. 6C). However, the interaction
534 between temperature and pH did not significantly affect shell birefringence at 72 hpf ($F_{1,8} = 0.08$,
535 $p = 0.784$; Fig. 6D).



536

537 **Fig. 6** Individual effects of pH and temperature on mean shell birefringence of larvae at **A)** 24
 538 hpf and **C)** 72 hpf (n = 6 tanks per treatment). Combined effects of pH and temperature on mean
 539 shell birefringence of larvae at **B)** 24 hpf and **D)** 72 hpf (n = 3 tanks per treatment). bar values
 540 represent means and error bars represent the standard deviation of the mean. Asterisks indicate
 541 significant differences between either temperature or pH treatments, as determined by two-way
 542 ANOVA.

543

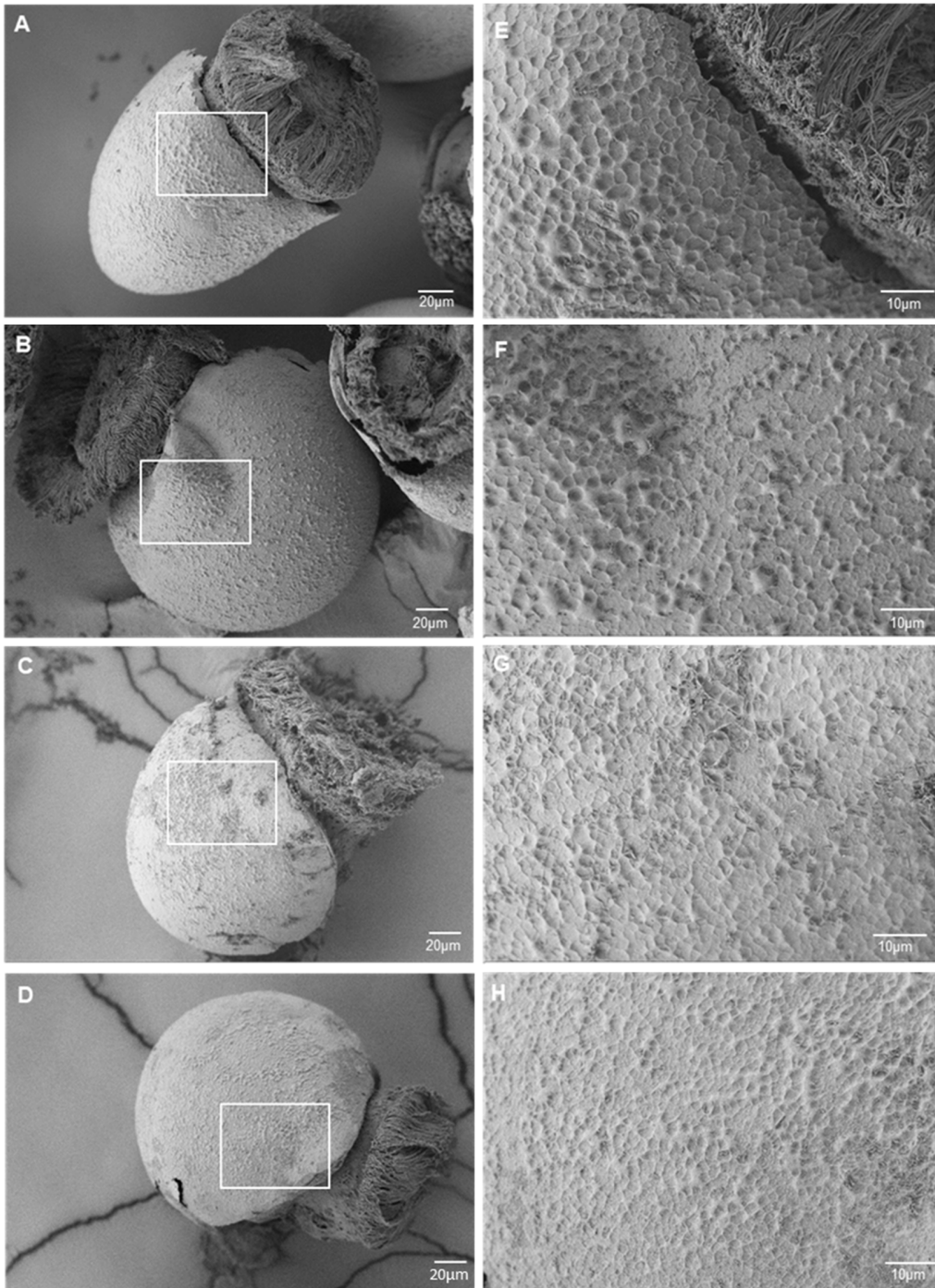
544

545

546

547 *Scanning electron microscopy*

548 In the high pH treatments (7.9), the shell surface of larvae observed at 24 hpf showed a normal
549 granular texture with an alveolar pattern (Fig. 7A, B, E, F). However, the larvae reared in the
550 low-pH treatments (7.6) showed signs of shell deformation and microfractures (Fig. 7C, D).
551 Details of the shell surface boxed in Figures 7C and 7D revealed irregularities and mineralization
552 defects that were probably due to shell dissolution. pH 8.0The shell surface of larvae observed at
553 72 hpf were of similar shape and pattern in both the low (7.7) and high (8.0) pH treatments (Fig.
554 8A–D). At higher magnification, the shell surfaces of high pH larvae revealed a homogeneous
555 granular texture and alveolar pattern (Fig. 8E, F). In the low-pH treatments, the details of the
556 shell surface boxed in 8C and 8D revealed surface heterogeneities and small holes within the
557 alveolar network suggesting mineral dissolution. (Fig. 8G, H)



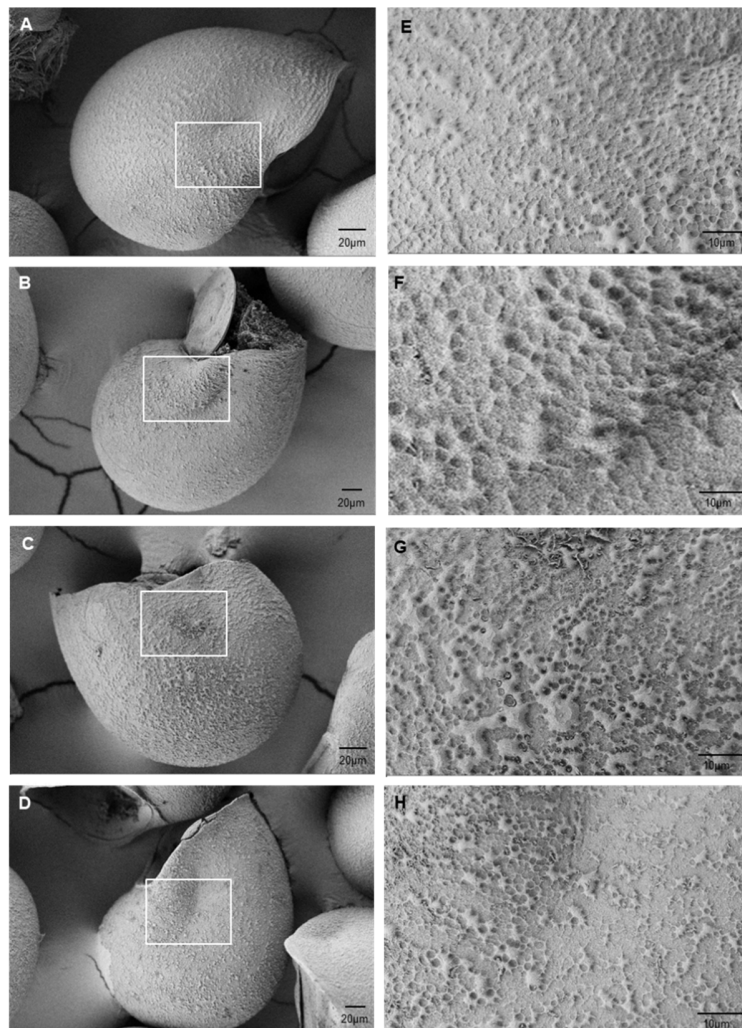
558

559 **Fig. 7** Scanning electron microscopy (SEM) images of *Haliotis tuberculata* larvae at 24 hpf in
 560 the four experimental treatments **A)** pH 8.0–17°C; **B)** pH 8.0–19°C; **C)** pH 7.7–17°C; and **D)** pH

561 7.7–19°C. Lateral views of the larvae show the protoconch shell and the velum. **E–H** show
562 magnified views of the corresponding white squares in A–D.

563

564 The shell surface of larvae observed at 72 hpf were of similar shape and pattern in both the low
565 (7.7) and high (8.0) pH treatments (Fig. 8A–D). The magnified areas of the shells in all
566 treatments revealed a typical granular texture and alveolar pattern (Fig. 8E–H). However, the
567 surface heterogeneities and small holes within the alveolar network in the low-pH treatments
568 (Fig. 8G, H) suggest mineral dissolution.



569

570 **Fig. 8** Scanning electron microscopy (SEM) images of *Haliotis tuberculata* larvae at 72 hpf in
571 the four experimental treatments **A**) pH 8.0–17°C; **B**) pH 8.0–19°C; **C**) pH 7.7–17°C; and **D**) pH
572 7.7–19°C. Lateral views of the larvae show the well-developed protoconch covering the larval
573 body. In **A**, the protoconch is well developed and covers the larval body. In **B**, the operculum
574 closes the shell aperture after complete retraction of the veliger. **E–H** show magnified views of
575 the corresponding white squares in A–D.

576

577

578 *Larval behavior*

579 None of the larval behavioral parameters (Distance moved (total cm⁻¹), mean velocity (cm·ms⁻¹),
580 mean meander (deg·cm⁻¹) differed significantly due to pH, temperature, or the interaction
581 between pH and temperature (Table S3).

582

583

584

585 *Respiration rate*

586 The respiration rate of larvae did not differ significantly between pH ($F_{1,8} = 1.54$, $p = 0.250$; two-
587 way ANOVA), or temperature ($F_{1,8} = 2.57$, $p = 0.15$; two-way ANOVA). No interaction was
588 found between pH and temperature for larval respiration rate ($F_{1,8} = 5.66$, $p = 0.045$).

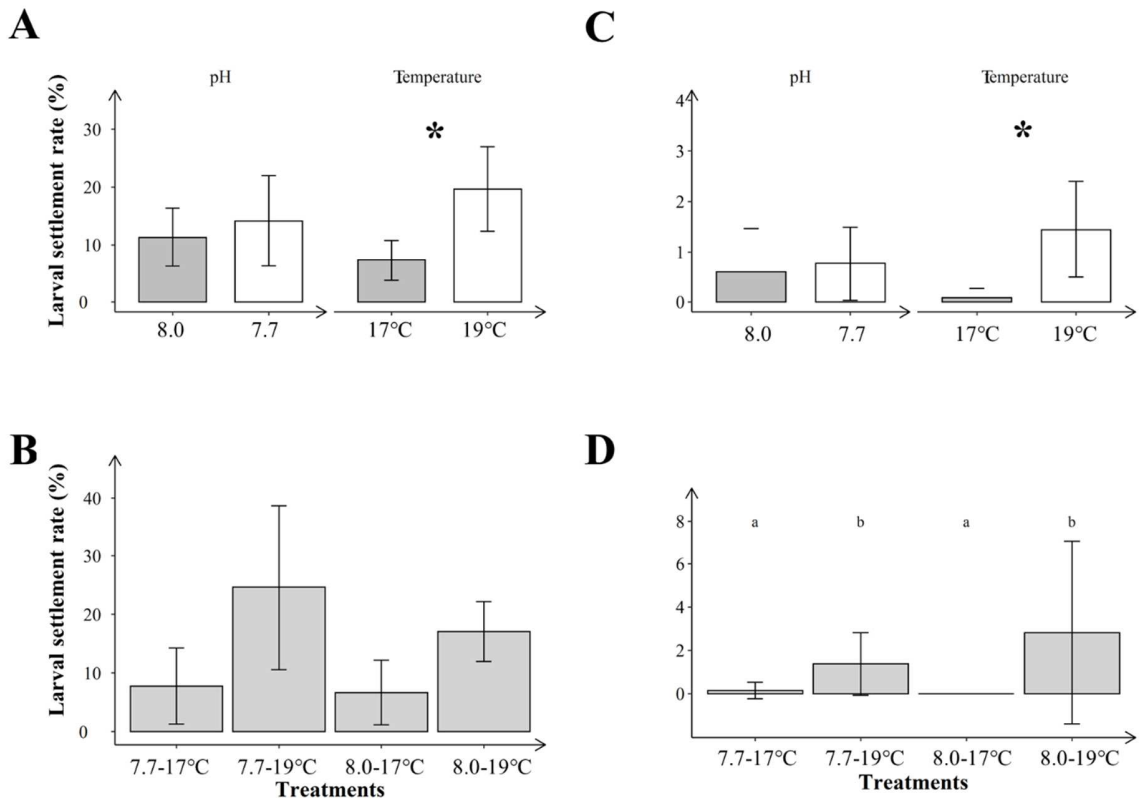
589

590

591 *Larval settlement*

592 The larval settlement on *Ulvelia*-covered plates was significantly higher in the high temperature
593 (19°C) treatments than in the low temperature (17°C) treatments ($F_{1,7} = 14.02$, $p = 0.007$; Fig.
594 9A). No significant differences were observed between pH treatments ($F_{1,7} = 1.40$, $p = 0.275$;
595 Fig. 9A) or from the interaction between pH and temperature ($F_{1,7} = 0.47$, $p = 0.52$; Fig. 9C).

596 On blank plates, we found significant effects from temperature ($W = 0$, $p = 0.005$; Wilcoxon rank
597 sum test with continuity correction; Fig. 9C) and from the four treatment comparisons ($H(3) =$
598 8.70 , $p = 0.033$; Kruskal–Wallis) (Fig. 9D). Larval settlement on the blank plates was
599 significantly higher in the high temperature (19°C) treatments than in the low temperature (17°C)
600 treatments (Fig. 9B). No significant differences were found between the low-pH and high pH
601 treatments ($W = 14$, $p = 0.923$; Wilcoxon rank sum test with continuity correction; Fig. 9C).



602

603

604

605

606

607

608

609

610

611

612

Fig. 9 Effects of pH and temperature on larval settlement on **A**) plates covered with the green microalga *Ulvella lens* (n = 6 tanks per treatment; two-way ANOVA) and **B**) blank plates (n = 6 tanks per treatment; Wilcoxon rank sum test with continuity correction). Combined effects of pH and temperature on larval settlement on **C**) *Ulvella*-covered plates and **D**) blank plates at 96 hours post-fertilization (hpf) (n = 3 tanks per treatment). bar values represent means and error bars represent the standard deviation of the mean. Different lowercase letters indicate significant differences among treatments. Asterisks indicate significant differences between either temperature or pH treatments.

613 **Discussion**

614 In this study, we exposed *H. tuberculata* larvae to the individual and combined effects of OA and
615 OW. We found that a 0.3-unit decrease in pH induced decreases in or no effects on larval
616 responses, whereas a 2°C increase in temperature caused broader effects, resulting in either
617 increased/enhanced, decreases/diminished larval responses or had no impacts. However, no
618 significant interactive effects of temperature and pH were observed for the variables measured.
619 Despite that, some treatment effects were recorded for the parameters that were not analyzed
620 using ANOVA (Table 3). Among the biological parameters investigated in this study, shell
621 formation, length, and calcification appeared to be the most sensitive to the effects of
622 temperature and pH. The results of this study lend further support to the results from recent
623 meta-analyses suggesting that the interactive effects of OA and OW on calcifying species,
624 including mollusks, are not as ubiquitous as OA's and OW's individual effects (Kroeker et al.,
625 2013; Przeslawski et al., 2015).

626 The hatching success of trochophore larvae of *H. tuberculata* was not significantly affected by
627 temperature, pH, or the interaction of the two. These results are in line with those of Pedroso
628 (2017), who found no impact on the hatching success of *H. asinina* in response to raising the
629 ambient temperature of 29°C by 2°C. The lack of significant effects by pH or by the interaction
630 of pH and temperature was likewise similar to previous findings. Guo et al. (2015) found no
631 effect of pH_{NBS} 7.94 on the hatching success of *H. diversicolor* and *H. discus*, whereas both
632 species experienced reduced hatching success when the pH value was decreased to 7.71 or
633 lower, compared with the high pH of 8.15. In two separate studies on the hatching success of *H.*
634 *discus hannai*, Kimura et al. (2011) and Li et al. (2013) found no impact of exposure to pH_{NBS}
635 7.6 and higher, compared with pH of 8.02. Likewise, Tahil and Dy (2016) found that pH_{NBS} 7.78

636 did not affect the *H. asinina* hatching success compared to the pH of 7.97; however, pH
637 treatments of 7.60 and 7.40 negatively affected the hatching success. Our results show that *H.*
638 *tuberculata* larvae can hatch at the lower pH values and high temperatures expected in the
639 coming decades. Such tolerance to OA and OW in the early larval stages has already been
640 reported for other marine species (Przeslawski et al., 2015), and might originate from protective
641 factors in the egg (Hamdoun and Epel, 2007).

642 An increased number of larvae with tissue abnormalities was observed under high temperature
643 treatments. This was accompanied by significant declines in the percentage of swimming larvae
644 in the high temperature treatments compared to the low temperature treatments at 24, 72 and 96
645 hpf. Low pH, also, reduced the normal tissue development of the larval stages. A study on *H.*
646 *asinina* found < 1% of normal trochophores at the reduced pH of 7.60, compared with the
647 ambient pH of 7.97 (Tahil and Dy, 2016). Parker et al. (2011) also reported slower larval
648 development in the Sydney rock oyster, *Saccostrea glomerata*, when the ambient pH (pH_{NBS} 8.2)
649 was reduced by 0.3 pH units. A study by Wessel et al. (2018) on *H. tuberculata* showed a
650 significant increase in the number of 30-hpf larvae with abnormal and delayed development at
651 pH_T 8.0 compared with larvae at pH_T 7.7 and 7.6. These findings suggest that a difference of only
652 a few hours of exposure to stressors can influence their effects during larval development.

653 Larval shell formation was also impaired under low pH, similar to previous studies on *H.*
654 *coccoradiata* (pH_{NBS} = 7.8 and 7.6 compared with the ambient pH of 8.2; Byrne et al., 2011); *H.*
655 *kamtschatkana* (reported as pCO₂ values of 800 μatm and 1800 μatm compared with a control of
656 400 μatm; Crim et al., 2011); *H. asinina* (pH_{NBS} = 7.85 and 7.65 compared with the ambient pH
657 of 8.15; Santander-De Leon et al., 2018); and *H. tuberculata* (pH_T = 7.68 and 7.58 compared
658 with the ambient pH of 8.00; Wessel et al., 2018). Shell calcification of *H. tuberculata* larvae

659 was also reduced under low pH, as shown by the decrease in birefringence intensity measured at
660 24 and 72 hpf. Additional SEM observations revealed differences in larval shell texture and the
661 presence of numerous small holes on the outer shell surface, suggesting that CaCO₃ dissolution
662 may be responsible for the reduced calcification seen in larvae raised at a lower pH. The lack of
663 calcification observed under cross-polarization microscopy and SEM is consistent with previous
664 results from Wessel et al. (2018), and provides further evidence that abalone larvae deposit less
665 CaCO₃ and produce more fragile and thinner shells when exposed to OA. Our results confirm, as
666 reported for numerous mollusk species, that the growing calcified shells of larval and juvenile
667 abalones are highly sensitive to OA (Gazeau et al., 2013; Przeslawski et al., 2015). Naturally
668 occurring *H. tuberculata* populations may be at greater risk from future pH reduction, as early
669 shell alterations may impair larval development and recruitment.

670 In this study, the impaired process of shell formation induced by low pH was mitigated by high
671 temperature, resulting in a higher proportion of 24- and 72-hpf larvae with normal shell
672 development as shown in Fig. 5A and 5C. Observations of temperature reducing the negative
673 impacts of OA on shell calcification and development have been previously reported for larval
674 and juvenile mollusks (Davis et al., 2013; Ko et al., 2014).

675 Shell length of *H. tuberculata* larvae was significantly reduced by low-pH conditions, but no
676 temperature or interaction effects were observed. Crim et al. (2011) reported a 5% reduction in
677 larval shell size in the northern abalone *H. kamtschatkana* after an 8-day exposure to acidified
678 conditions (reported as CO₂ levels 400 μatm vs 800 μatm), which is consistent with our results
679 (4% reduction at 24 hpf and 6% reduction at 72 hpf). Similarly, the larvae of *H. asinina* (pH_{NBS} =
680 7.85 and 7.65 compared with the ambient pH of 8.15; Santander-De Leon et al., 2018); *H.*
681 *diversicolor*; and *H. discus hannai* (pH_{NBS} = 7.94 and lower compared with the high pH of 8.15;

682 Guo et al., 2015) experienced reductions in shell length at low-pH compared with high pH
683 conditions. In a study by Onitsuka et al. (2018), larvae of *H. discus hannai* at pH_{NBS} 7.79 did not
684 show any significant reduction in shell length compared with larvae at the high pH_{NBS} of 7.99.

685 In our study, the lack of significant effects on shell size from temperature or from the interaction
686 between temperature and pH is consistent with results obtained for other marine mollusks. For
687 example, Thiyagarajan and Ko (2012) reported no impact of high temperature (30°C compared
688 with 24°C), or temperature–pH interaction on the shell size of the Portuguese oyster *Crassostrea*
689 *angulata*. On the other hand, Talmage and Gobler (2011) recorded decreased larval size in two
690 bivalves (*Mercenaria mercenaria* and *Argopecten irradians*) resulting from both a reduced
691 pH_{NBS} of 7.8 (compared with the ambient pH of 8.08) and an high temperature of 28°C
692 (compared with the ambient temperature of 24°C). These contrasting effects confirm a high
693 variability in the responses of marine mollusk larvae to both isolated and combined stressors.

694 The absence of direct effects of pH and temperature on larval physiology and behavior does not
695 rule out the existence of their indirect effects through cellular and molecular mechanisms that
696 were not measured in the present study. Indeed, larval developmental stages are characterized by
697 huge changes (in physiology and sensitivity) over a short period of time (5 days) and the
698 measurements of physiological and behavioral variables do not account for the whole
699 developmental processes that may be impacted by the stressors. Complementary studies at the
700 molecular level (i.e., gene expression, protein and enzyme synthesis, etc.) will be needed to fully
701 understand the fine developmental changes induced by the climate change drivers (Portner et al.
702 2010).

703

704 Larval settlement was greater at high temperatures than at the low temperature on both *Ulvel*-
705 covered and blank plates. The shorter larval duration that corresponded with high temperature in
706 this study is consistent with previous studies of related *Haliotis* species, such as *H. sorenseni*, *H.*
707 *rufescens*, *H. corrugata*, and *H. fulgens* (Leighton, 1972, 1974). This suggests that high
708 temperatures resulting from global warming reduce the duration of the planktonic larval stage
709 and accelerate the settlement rate (Byrne et al., 2011). This may be an advantage (Byrne et al.,
710 2011), as a longer planktonic stage may reduce the chances of survival due to increased risk of
711 predation and exposure to other environmental stresses (Parker et al., 2013). We did not record
712 any significant effects of pH on *H. tuberculata* settlement, which is in line with the findings of
713 another study on *H. kamtschatkana* (Crim et al., 2011). However, the literature contains
714 contradictory results, with a tendency toward a lower settlement rate of the New Zealand
715 abalone, *H. iris*, in low-pH conditions (Espinel-Velasco et al., 2020) as well as for the donkey's
716 ear abalone, *H. asinina*, in three low-pH treatments (Tahil and Dy, 2015).

717 Our results showed that in every treatment, the settlement rate of *H. tuberculata* larvae on
718 *Ulvel*-covered plates was higher than the settlement rate on blank plates by a factor of at least
719 15. This supports the notion that settlement cues increase marine invertebrate larval settlement
720 (Hadfield and Paul, 2001; Pawlik, 1992; Rodriguez et al., 1993). However, lowered pH may
721 cause indirect effects, due to the effect of low pH on the settlement substrate. For example,
722 O'Leary et al. (2017) reported that the settlement rate of *H. rufescens* under both present-day and
723 low-pH treatments increased from 11% in tanks with no crustose coralline algae, to ~70% in the
724 presence of crustose coralline algae. This raises another concern regarding the indirect impacts of
725 OA and OW on abalone larval settlement. Coralline algae are common settlement cues for
726 abalone larvae (De Viçose et al., 2010, 2012; Williams et al., 2008; Roberts et al., 2004; Roberts

727 and Nicholson, 1997), and they are decreasing due to OA and OW (Kuffner et al., 2008; Martin
728 and Gattuso, 2009; Diaz-Pulido et al., 2012; Hofmann et al., 2012). Therefore, even in the
729 absence of the direct impacts of OA and OW on abalone larvae, such environmental changes
730 may indirectly reduce larval settlement by reducing their settlement cues. On the other hand, if
731 *Ulvelia* species, like many non-calcifying macroalgae, can benefit from high temperatures and
732 reduced pH (Koch et al., 2013; Hofmann et al., 2012), then abalone larvae may be able to
733 maintain their normal settlement rates. This presents an area requiring further examination.

734 None of the other behavioral responses (Distance moved (total cm^{-1}), mean velocity ($\text{cm}\cdot\text{ms}^{-1}$),
735 mean meander ($\text{deg}\cdot\text{cm}^{-1}$),) differed as an effect of pH, temperature, or the interaction between
736 the two. These outcomes parallel the responses of 2-day-old larvae of the Pacific oyster,
737 *Crassostrea gigas*, when exposed to high pH and low (-0.3 units) pH conditions (Valentini,
738 2019). Although the method used in this research to study larval behavior is very common, it is
739 noted that applying such a two-dimensional method may not allow the abalone larvae to express
740 natural swimming behavior. Therefore, developing three dimensional methods are desired for
741 future studies.

742 The lack of significant changes in larval behavior may partly justify the lack of changes observed
743 in larval respiration. Larval respiration of *H. tuberculata* did not differ due to the individual or
744 combined factors of pH and temperature. Although very low pH and highly high temperatures
745 (i.e., out of the projected ranges for the year 2100) are known to amplify respiration (Campanati
746 et al., 2018; Waldbusser et al., 2015; Liu and He, 2012; Padilla-Gamiño et al., 2013), some
747 studies have confirmed that respiration was not impacted by a -0.3 unit pH reduction and/or a
748 $+3^{\circ}\text{C}$ temperature increase above the ambient conditions (Frieder et al., 2017). For example, the
749 respiration rate of the larvae of *Mytilus californianus* did not change when the ambient pH was

750 reduced from 8.3 to 7.8 (Waldbusser et al., 2015). Similarly, Campanati et al. (2018) found no
 751 impact on the oxygen consumption of *Reishia clavigera* larvae when the ambient pH was
 752 reduced from 8.1 to 7.6. High pCO₂ in seawater likely increases the maintenance costs of acid–
 753 base homeostasis, the intracellular ion balance required for protein folding and pH-sensitive
 754 physiological processes (Rivest and Hofmann, 2014; Lefevre, 2016). Therefore, our observation
 755 in this study of a lack of increase in *H. tuberculata* metabolic rates under acidified conditions
 756 may suggest that the larvae were able to use existing pools of ion pumps to conserve their acid–
 757 base homeostasis (Portner and Reipschlager, 1996; Guppy and Withers, 1999).

758

759 **Table 3** Full results summary showing the effects of temperature, pH, and their interaction on
 760 the various parameters observed during this study. Arrow direction indicates whether these
 761 factors decreased/diminished (↓), increased/enhanced (↑), or had no significant effect (ns) on the
 762 measured parameters of *H. tuberculata* at 24, 72, and 96 hours post-fertilization (hpf). Empty
 763 cells indicate that the corresponding results were not applicable because they were not measured.
 764 Where nonparametric tests were used (i.e., for shell formation and tissue formation), treatment
 765 impacts are shown instead of interaction effects.

Parameter	Temperature effect			pH effect			Interaction effect		
	24 hpf	72 hpf	96 hpf	24 hpf	72 hpf	96 hpf	24 hpf	72 hpf	96 hpf
Hatching success	ns			ns			ns		
Percentage of swimming larvae	↓	↓	↓	ns	ns	ns	ns	ns	ns

Shell formation	↑	↓		↓	↓		8.0 - 17°C = ambient 7.7 - 19°C =↓ 8.0 - 19°C = ↑ 7.7 - 17°C =↓	8.0 - 17°C = ambient 7.7 - 19°C =↓ 8.0 - 19°C = ns 7.7 - 17°C =↓	
Tissue formation	↓	ns		↓	↓		8.0 - 17°C = ambient 7.7 - 19°C = ↓ 8.0 - 19°C = ↓ 7.7 - 17°C = ns	8.0 - 17°C = ambient 7.7 - 19°C = ↓ 8.0 - 19°C = ns 7.7 - 17°C = ↓	
Shell length		ns			↓			ns	
Shell calcification	ns	↓		↓	↓		ns	ns	
Respiration rate		ns			ns			ns	
Larval swimming behaviors		ns			ns			ns	
Larval settlement			↑			ns			ns

766

767 In conclusion, the majority of the responses of *H. tuberculata* larvae were affected by low pH
768 and high temperature, but not by their interactions as summarized in Table 3. We did not detect
769 any significant interaction between the high temperature and low-pH stressors. However, such
770 interactions may exist, but we were not able to detect them using non-parametric tests. . For
771 example, although high temperature accelerated shell formation at 24 hpf, this was partially
772 mitigated by low pH. High temperature, however, turned into a threat by increasing the larval
773 tissue malformation at 24 hpf. High temperature decreased the percentage of swimming larvae at

774 all stages. It also declined shell calcification at 72 hpf despite the fact that it did not affect that of
775 larvae at 24 hpf. By the end of the larval stage at 96 hpf, high temperature accelerated the larval
776 settlement rate, which might reduce its detrimental effects on larval survival. Low pH, however,
777 did not have any impact on the larval settlement. Low pH impaired all shell formation related
778 parameters in all stages. However, like high temperature, it did not affect processes such as
779 hatching success, respiration rate and swimming behaviors. Even though the projected rates of
780 pH decrease and temperature increase over the coming decades may not seem to be an obstacle
781 for *H. tuberculata* larval production, it seems that under OA and OW, the majority of this
782 species' responses are susceptible to changes in either temperature or pH. Thus, *H. tuberculata*
783 larvae will have to cope with both stressors. In nature, this may happen through adaptation. In
784 abalone farms, this can occur using various strategies. For example, first, by monitoring of the
785 daily changes in seawater pH, it can be arranged to and adjustment of avoid pumping low pH
786 seawater into the farms when during the hours when the CO₂ concentrations in the seawater is at
787 its peak ion (Murie and Bourdeau 2020). If farms have access to large-volume storage tanks,
788 adding kelp species to the tanks may reduce CO₂ concentrations as kelp canopies have the
789 ability to alter local seawater chemistry (Murie and Bourdeau 2020). Inclusion of an integrated
790 multi-trophic aquaculture system based on algae might be helpful (Bolton et al. 2009) Addition
791 of chemicals to increase seawater alkalinity and/or pH might be another solution for the
792 hatcheries with a recirculating system. The selection of tolerant broodstocks to OA and GW can
793 be also undertaken. However, due to the limitations of each of the aforementioned methods, the
794 combinations of them may lead to more sustainable abalone productions.

795

796

797 **Acknowledgements**

798 JK was supported by a post-doctoral fellowship from the French government under the program
799 "*Investissements d'Avenir*", co-funded by the ISblue project "*Interdisciplinary graduate school*
800 *for the blue planet*" (ANR-17-EURE-0015). This work was supported in part by the program
801 "*Acidification des Océans*" (ICOBio project) funded by the *Fondation pour la Recherche sur la*
802 *Biodiversité* (FRB) and the *Ministère de la Transition Ecologique et Solidaire* (MTES). The
803 Regional Council of Brittany, the General Council of Finistère, the urban community of
804 Concarneau Cornouaille Agglomération and the European Regional Development Fund (ERDF)
805 are acknowledged for the funding of the scanning electron microscope (Sigma 300 FE-SEM) at
806 the Concarneau Marine Station. Philippe Dubois is a Research Director of the National Fund for
807 Scientific Research (Belgium). We thank Stéphane Formosa for his assistance in SEM (*Plateau*
808 *technique de Microscopie Electronique du Muséum National d'Histoire Naturelle, Concarneau,*
809 France). We thank all the staff of the France *Haliotis* farm (Plouguerneau) for hosting the
810 experiment.

811

812 **References**

813 Alter, K., Andrewartha, S.J., Clark, T.D., Elliott, N.G., 2017. Thermal preference increases during larval
814 development of pure and hybrid abalone. *J. Shellfish Res.* 36, 141-149.

815 Auzoux-Bordenave, S., Badou, A., Gaume, B., Berland, S., Helléouet, M.-N., Milet, C., Huchette, S.,
816 2010. Ultrastructure, chemistry and mineralogy of the growing shell of the European abalone
817 *Haliotis tuberculata*. *J. Struct. Biol* 171, 277-290.

818 Auzoux-Bordenave, S., Wessel, N., Badou, A., Martin, S., M'zoudi, S., Avignon, S., Roussel, S.,
819 Huchette, S., Dubois, P., 2020. Ocean acidification impacts growth and shell mineralization in
820 juvenile abalone (*Haliotis tuberculata*). Mar. Biol. 167, 1-14.

821 Avignon, S., Auzoux-Bordenave, S., Martin, S., Dubois, P., Badou, A., Coheleach, M., Richard, N., Di
822 Giglio, S., Malet, L., Servili, A., 2020. An integrated investigation of the effects of ocean
823 acidification on adult abalone (*Haliotis tuberculata*). ICES J. Mar. Sci. 77, 757-772.

824 Bennett, C.E., Marshall, D.J., 2005. The relative energetic costs of the larval period, larval swimming and
825 metamorphosis for the ascidian *Diplosoma listerianum*. Mar. Freshwat. Behav. Physiol. 38, 21-29.

826 Bolton, J.J., Robertson-Andersson, D.V., Shuuluka, D., Kandjengo, L., 2009. Growing *Ulva*
827 (Chlorophyta) in integrated systems as a commercial crop for abalone feed in South Africa: a SWOT
828 analysis. J. Appl. Phycol. 21, 575-583.

829 Byrne, M., Ho, M., Wong, E., Soars, N.A., Selvakumaraswamy, P., Shepard-Brennand, H., Dworjanyn,
830 S.A., Davis, A.R., 2011. Unshelled abalone and corrupted urchins: development of marine calcifiers
831 in a changing ocean. Proc Biol Sci 278, 2376-2383. doi: 10.1098/rspb.2010.2404.

832 Byrne, M., Przeslawski, R., 2013. Multistressor impacts of warming and acidification of the ocean on
833 marine invertebrates' life histories. Integr. Comp. Biol. 53, 582-596. doi: 10.1093/icb/ict049.

834 Campanati, C., Dupont, S., Williams, G.A., Thiyagarajan, V., 2018. Differential sensitivity of larvae to
835 ocean acidification in two interacting mollusc species. Mar. Environ. Res. 141, 66-74. doi:
836 10.1016/j.marenvres.2018.08.005.

837 Cook, P.A., 2016. Recent trends in worldwide abalone production. Journal of Shellfish Research, 35:
838 581-583.

839 Crim, R.N., Sunday, J.M., Harley, C.D.G., 2011. Elevated seawater CO₂ concentrations impair larval
840 development and reduce larval survival in endangered northern abalone (*Haliotis kamtschatkana*). J.
841 Exp. Mar. Biol. Ecol. 400, 272-277. doi: 10.1016/j.jembe.2011.02.002.

842 Daume, S., Brand-Gardner, S., Woelkerling, W.J., 1999. Preferential settlement of abalone larvae: diatom
843 films vs. non-geniculate coralline red algae. *Aquaculture* 174, 243-254. doi: 10.1016/s0044-
844 8486(99)00003-4.

845 Daume, S., Huchette, S., Ryan, S., Day, R.W., 2004. Nursery culture of *Haliotis rubra*: the effect of
846 cultured algae and larval density on settlement and juvenile production. *Aquaculture* 236, 221-239.
847 doi: 10.1016/j.aquaculture.2003.09.035.

848 Davis, A.R., Coleman, D., Broad, A., Byrne, M., Dworjanyn, S.A., Przeslawski, R., 2013. Complex
849 responses of intertidal molluscan embryos to a warming and acidifying ocean in the presence of UV
850 radiation. *PLoS One* 8, e55939-e55939. doi: 10.1371/journal.pone.0055939.

851 De Viçose, G.C., Viera, M.P., Huchette, S., Izquierdo, M.S., 2012. Larval settlement, early growth and
852 survival of *Haliotis tuberculata coccinea* using several algal cues. *J. Shellfish Res.* 31, 1189-1198.
853 doi: 10.2983/035.031.0430.

854 Diaz-Pulido, G., Anthony, K.R.N., Kline, D.I., Dove, S., Hoegh-Guldberg, O., 2011. Interactions between
855 ocean acidification and warming on the mortality and dissolution of coralline algae1. *J. Phycol.* 48,
856 32-39. doi: 10.1111/j.1529-8817.2011.01084.x.

857 Dickson, A.G., Millero, F.J., 1987. A comparison of the equilibrium constants for the dissociation of
858 carbonic acid in seawater media. *Deep Sea Research Part A. Oceanographic Research Papers* 34,
859 1733-1743. doi: 10.1016/0198-0149(87)90021-5.

860 Dickson, A.G., Sabine, C.L., Christian, J.R., 2007. Guide to best practices for ocean CO₂ measurements.
861 North Pacific Marine Science Organization.

862 Doney, S.C., Fabry, V.J., Feely, R.A., Kleypas, J.A., 2009. Ocean acidification: The other CO₂ problem.
863 *Annual Review of Marine Science* 1, 169-192. doi: 10.1146/annurev.marine.010908.163834.

864 Feely, R.A., 2004. Impact of anthropogenic CO₂ on the CaCO₃ system in the oceans. *Science* 305, 362-
865 366. doi: 10.1126/science.1097329.

866 Fernández-Reiriz, M.J., Range, P., Álvarez-Salgado, X.A., Espinosa, J., Labarta, U., 2012. Tolerance of
867 juvenile *Mytilus galloprovincialis* to experimental seawater acidification. *Mar. Ecol. Prog. Ser.* 454,
868 65-74. doi: 10.3354/meps09660.

869 Fonseca, J.G., Laranjeiro, F., Freitas, D.B., Oliveira, I.B., Rocha, R.J.M., Machado, J., Hinzmann, M.,
870 Barroso, C.M., Galante-Oliveira, S., 2020. Impairment of swimming performance in *Tritia reticulata*
871 (L.) veligers under projected ocean acidification and warming scenarios. *Sci. Total Environ.* 731,
872 139187. doi: 10.1016/j.scitotenv.2020.139187.

873 Frieder, C.A., Applebaum, S.L., Pan, T.C.F., Hedgecock, D., Manahan, D.T., 2016. Metabolic cost of
874 calcification in bivalve larvae under experimental ocean acidification. *ICES J. Mar. Sci.* 74, 941-954.
875 doi: 10.1093/icesjms/fsw213.

876 Gao, K., Gao, G., Wang, Y., Dupont, S., 2020. Impacts of ocean acidification under multiple stressors on
877 typical organisms and ecological processes. *Marine Life Science & Technology* 2, 279-291. doi:
878 10.1007/s42995-020-00048-w.

879 Gilroy, A., Edwards, S.J., 1998. Optimum temperature for growth of Australian abalone: preferred
880 temperature and critical thermal maximum for blacklip abalone, *Haliotis rubra* (Leach), and greenlip
881 abalone, *Haliotis laevigata* (Leach). *Aquacult. Res.* 29, 481-485. doi: 10.1111/j.1365-
882 2109.1998.tb01157.x.

883 Green, B.S., Fisher, R., 2004. Temperature influences swimming speed, growth and larval duration in
884 coral reef fish larvae. *J. Exp. Mar. Biol. Ecol.* 299, 115-132. doi: 10.1016/j.jembe.2003.09.001.

885 Guo, X., Huang, M., Pu, F., You, W., Ke, C., 2015. Effects of ocean acidification caused by rising CO₂
886 on the early development of three mollusks. *Aquatic Biology* 23, 147-157. doi: 10.3354/ab00615.

887 Guppy, M., Withers, P., 1999. Metabolic depression in animals: physiological perspectives and
888 biochemical generalizations. *Biol. Rev. Camb. Philos. Soc.* 74, 1-40. doi:
889 10.1017/s0006323198005258.

890 Hadfield, M., Paul, V., 2001. Natural chemical cues for settlement and metamorphosis of marine-
891 invertebrate larvae, *Marine Science*. CRC Press, pp. 431-461.

892 Hamdoun, A., Epel, D., 2007. Embryo stability and vulnerability in an always changing world. Proc Natl
893 Acad Sci U S A 104, 1745-1750. doi: 10.1073/pnas.0610108104.

894 Harney, E., Lachambre, S., Roussel, S., Huchette, S., Enez, F., Morvezen, R., Haffray, P., Boudry, P.,
895 2018. Transcriptome based SNP discovery and validation for parentage assignment in hatchery
896 progeny of the European abalone *Haliotis tuberculata*. Aquaculture 491, 105-113. doi:
897 10.1016/j.aquaculture.2018.03.006.

898 Hofmann, L.C., Straub, S., Bischof, K., 2012. Competition between calcifying and noncalcifying
899 temperate marine macroalgae under elevated CO2 levels. Mar. Ecol. Prog. Ser. 464, 89-105. doi:
900 10.3354/meps09892.

901 Huchette, S., 2004. Maternal variability in the blacklip abalone, *Haliotis rubra* leach (Mollusca:
902 Gastropoda): effect of egg size on fertilisation success. Aquaculture 231, 181-195. doi:
903 10.1016/j.aquaculture.2003.08.027.

904 Huchette, S., Clavier, J., 2004. Status of the ormer (*Haliotis tuberculata* L.) industry in Europe. J.
905 Shellfish Res. 23, 951-956.

906 IPCC, 2014. Summary for Policymakers. In: Climate Change 2014: Impacts, Adaptation, and
907 Vulnerability. Part A: Global and Sectoral Aspects. Contribution of Working Group II to the Fifth
908 Assessment Report of the Intergovernmental Panel on Climate Change. Cambridge University Press,
909 Cambridge, United Kingdom and New York, NY, USA, 1132 pp. Jardillier, E., Rousseau, M.,
910 Gendron-Badou, A., Fröhlich, F., Smith, D.C., Martin, M., Helléouet, M.N., Huchette, S., Doumenc,
911 D., Auzoux-Bordenave, S., 2008. A morphological and structural study of the larval shell from the
912 abalone *Haliotis tuberculata*. Mar. Biol. 154, 735-744. doi: 10.1007/s00227-008-0966-3.

913 Kashiwada, J.V., Taniguchi, I.K., 2007. Application of recent red abalone *Haliotis rufescens* surveys to
914 management decisions outlined in the california abalone recovery and management plan. J. Shellfish
915 Res. 26, 713-717. doi: 10.2983/0730-8000(2007)26[713:aorrah]2.0.co;2.

916 Kimura, R.Y.O., Takami, H., Ono, T., Onitsuka, T., Nojiri, Y., 2011. Effects of elevated pCO₂ on the
917 early development of the commercially important gastropod, Ezo abalone *Haliotis discus hannai*.
918 Fish. Oceanogr. 20, 357-366. doi: 10.1111/j.1365-2419.2011.00589.x.

919 Ko, G.W.K., Dineshram, R., Campanati, C., Chan, V.B.S., Havenhand, J., Thiyagarajan, V., 2014.
920 Interactive effects of ocean acidification, elevated temperature, and reduced salinity on early-life
921 stages of the pacific oyster. Environ. Sci. Technol. 48, 10079-10088. doi: 10.1021/es501611u.

922 Koch, M., Bowes, G., Ross, C., Zhang, X.-H., 2012. Climate change and ocean acidification effects on
923 seagrasses and marine macroalgae. Global Change Biol. 19, 103-132. doi: 10.1111/j.1365-
924 2486.2012.02791.x.

925 Kroeker, K.J., Kordas, R.L., Crim, R., Hendriks, I.E., Ramajo, L., Singh, G.S., Duarte, C.M., Gattuso, J.-
926 P., 2013. Impacts of ocean acidification on marine organisms: quantifying sensitivities and
927 interaction with warming. Global Change Biol. 19, 1884-1896. doi: 10.1111/gcb.12179.

928 Kuffner, I.B., Andersson, A.J., Jokiel, P.L., Rodgers, K.u.S., Mackenzie, F.T., 2008. Decreased
929 abundance of crustose coralline algae due to ocean acidification. Nature Geoscience 1, 114-117. doi:
930 10.1038/ngeo100.

931 Kurihara, H., Kato, S., Ishimatsu, A., 2007. Effects of increased seawater pCO₂ on early development of
932 the oyster *Crassostrea gigas*. Aquatic Biology 1, 91-98. doi: 10.3354/ab00009.

933 Lafferty, K.D., Kuris, A.M., 1993. Mass mortality of abalone *Haliotis cracherodii* or the California
934 Channel Islands: tests of epidemiological hypothesis. Mar. Ecol. Prog. Ser. 96, 239-248. doi:
935 10.3354/meps096239.

936 Lannig, G., Eilers, S., Pörtner, H.O., Sokolova, I.M., Bock, C., 2010. Impact of ocean acidification on
937 energy metabolism of oyster, *Crassostrea gigas*--changes in metabolic pathways and thermal
938 response. Mar. Drugs 8, 2318-2339. doi: 10.3390/md8082318.

939 Lefevre, S., 2016. Are global warming and ocean acidification conspiring against marine ectotherms? A
940 meta-analysis of the respiratory effects of elevated temperature, high CO₂ and their interaction.
941 Conserv Physiol 4, cow009-cow009. doi: 10.1093/conphys/cow009.

942 Leighton, D.L., 1974. The influence of temperature on larval and juvenile growth in three species of
943 southern California abalones. *Fish. Bull.* 72, 1137-1145.

944 Lewis, E., Wallace, D.W.R., Lewis, E., 2011. Program developed for CO₂ system calculations, Carbon
945 Dioxide Information Analysis Center. ORNL Environmental Sciences Division.

946 Li, J., Jiang, Z., Zhang, J., Qiu, J.-W., Du, M., Bian, D., Fang, J., 2013. Detrimental effects of reduced
947 seawater pH on the early development of the Pacific abalone. *Mar. Pollut. Bull.* 74, 320-324. doi:
948 10.1016/j.marpolbul.2013.06.035.

949 Liu, W., He, M., 2012. Effects of ocean acidification on the metabolic rates of three species of bivalve
950 from southern coast of China. *Chin. J. Oceanol. Limnol.* 30, 206-211. doi: 10.1007/s00343-012-
951 1067-1.

952 Lu, J., Lin, Q., Sun, Y., Sheng, J., Chen, Q., 2004. Effect of temperature on the early development of
953 *Haliotis diversicolor Reeve*. *J. Shellfish Res.* 23, 963-967.

954 Martin, S., Gattuso, J.-P., 2009. Response of Mediterranean coralline algae to ocean acidification and
955 elevated temperature. *Global Change Biol.* 15, 2089-2100. doi: 10.1111/j.1365-
956 2486.2009.01874.x. Mehrbach, C., Culberson, C.H., Hawley, J.E., Pytkowicz, R.M., 1973.
957 Measurement of the apparent dissociation constants of carbonic acid in seawater at atmospheric
958 pressure. *Limnol. Oceanogr.* 18, 897-907. doi: 10.4319/lo.1973.18.6.0897.

959 Micheli, F., Shelton, A.O., Bushinsky, S.M., Chiu, A.L., Haupt, A.J., Heiman, K.W., Kappel, C.V.,
960 Lynch, M.C., Martone, R.G., Dunbar, R.B., Watanabe, J., 2008. Persistence of depleted abalones in
961 marine reserves of central California. *Biol. Conserv.* 141, 1078-1090. doi:
962 10.1016/j.biocon.2008.01.014.

963 Morales-Bojórquez, E., Muciño-Díaz, M.O., Vélez-Barajas, J.A., 2008. Analysis of the decline of the
964 abalone fishery (*Haliotis fulgens* and *H. corrugata*) along the westcentral coast of the Baja California
965 peninsula, Mexico. *J. Shellfish Res.* 27:865–870.

966 Morash, A.J., Alter, K., 2015. Effects of environmental and farm stress on abalone physiology:
967 perspectives for abalone aquaculture in the face of global climate change. *Rev Aquacult* 7:1–27.

968 Nagelkerken, I., Munday, P.L., 2015. Animal behaviour shapes the ecological effects of ocean
969 acidification and warming: moving from individual to community-level responses. *Global Change*
970 *Biol.* 22, 974-989. doi: 10.1111/gcb.13167.

971 Narita, D., Rehdanz, K., Tol, R.S.J., 2012. Economic costs of ocean acidification: a look into the impacts
972 on global shellfish production. *Clim. Change* 113, 1049-1063. doi: 10.1007/s10584-011-0383-3.

973 O'Leary, J.K., Barry, J.P., Gabrielson, P.W., Rogers-Bennett, L., Potts, D.C., Palumbi, S.R., Micheli, F.,
974 2017. Calcifying algae maintain settlement cues to larval abalone following algal exposure to
975 extreme ocean acidification. *Sci Rep* 7, 1-10.

976 Onitsuka, T., Takami, H., Muraoka, D., Matsumoto, Y., Nakatsubo, A., Kimura, R., Ono, T., Nojiri, Y.,
977 2018. Effects of ocean acidification with pCO₂ diurnal fluctuations on survival and larval shell
978 formation of Ezo abalone, *Haliotis discus hannai*. *Mar. Environ. Res.* 134, 28-36. doi:
979 10.1016/j.marenvres.2017.12.015.

980 Padilla-Gamiño, J.L., Kelly, M.W., Evans, T.G., Hofmann, G.E., 2013. Temperature and CO₂ additively
981 regulate physiology, morphology and genomic responses of larval sea urchins, *Strongylocentrotus*
982 *purpuratus*. *Proc Biol Sci* 280, 20130155-20130155. doi: 10.1098/rspb.2013.0155.

983 Parker, L.M., Ross, P.M., O'Connor, W.A., Pörtner, H.O., Scanes, E., Wright, J.M., 2013. Predicting the
984 response of molluscs to the impact of ocean acidification. *Biology (Basel)* 2, 651-692. doi:
985 10.3390/biology2020651.

986 Parker, L.M., Ross, P.M., O'Connor, W.A., Borysko, L., Raftos, D.A. Pörtner, H.O., 2012. Adult
987 exposure influences offspring response to ocean acidification in oysters. *Glob. Change Biol.* 18, 82-
988 92.

989 Pawlik, J.R., 1992. Chemical ecology of the settlement of benthic marine invertebrates. *Oceanogr. Mar.*
990 *Biol. Annu. Rev.*

991 Pedroso, F.L., 2017. Effects of elevated temperature on the different life stages of tropical mollusk,
992 donkey's ear abalone (*Haliotis asinina*). *Aquaculture, Aquarium, Conservation & Legislation*, 10,
993 1421-1427.

994 Pörtner, H., 2008. Ecosystem effects of ocean acidification in times of ocean warming: a physiologist's
995 view. *Mar. Ecol. Prog. Ser.* 373, 203-217. doi: 10.3354/meps07768.

996 Pörtner, H.O., 2010. Oxygen- and capacity-limitation of thermal tolerance: a matrix for integrating
997 climate-related stressor effects in marine ecosystems. *J. Exp. Biol.* 213, 881-893. doi:
998 10.1242/jeb.037523.

999 Przeslawski, R., Byrne, M., Mellin, C., 2015. A review and meta-analysis of the effects of multiple
1000 abiotic stressors on marine embryos and larvae. *Glob. Change Biol.* 21, 2122-2140.

1001 Qui-Minet, Z.N., Delaunay, C., Grall, J., Six, C., Cariou, T., Bohner, O., Legrand, E., Davoult, D.,
1002 Martin, S., 2018. The role of local environmental changes on maerl and its associated non-calcareous
1003 epiphytic flora in the Bay of Brest. *Estuarine. Coast. Shelf Sci.* 208, 140-152

1004 Rivest, E.B., Hofmann, G.E., 2014. Responses of the metabolism of the larvae of *Pocillopora damicornis*
1005 to ocean acidification and warming. *PLoS One* 9, e96172-e96172. doi:
1006 10.1371/journal.pone.0096172.

1007 Roberts, R.D., Kaspar, H.F., Barker, R.J., 2004. Settlement of abalone (*Haliotis iris*) larvae in response to
1008 five species of coralline algae. *J. Shellfish Res.* 23, 975-988.

1009 Roberts, R.D., Nicholson, C.M., 1997. Variable response from abalone larvae (*Haliotis iris*, *H. virginea*)
1010 to a range of settlement cues. *Molluscan Res.* 18, 131-141. doi: 10.1080/13235818.1997.10673687.

1011 Rodriguez, S.R., Ojeda, F.P., Inestrosa, N.C., 1993. Settlement of benthic marine invertebrates. *Mar.*
1012 *Ecol. Prog. Ser.* 97, 193-207. doi: 10.3354/meps097193.

1013 Rosenberg, G., 2014. A new critical estimate of named species-level diversity of the recent mollusca. *Am.*
1014 *Malacol. Bull.* 32, 308. doi: 10.4003/006.032.0204.

1015 Santander, S.M.S., 2018. CO₂-induced pH reduction hinders shell development of early larvae donkey's
1016 ear abalone *Haliotis asinina* (Linnaeus 1758). *Asian Fish. Sci.* 31. doi: 10.33997/j.afs.2018.31.2.002.

1017 Schalkhauser, B., Bock, C., Stemmer, K., Brey, T., Pörtner, H.-O., Lannig, G., 2012. Impact of ocean
1018 acidification on escape performance of the king scallop, *Pecten maximus*, from Norway. *Mar. Biol.*
1019 160, 1995-2006. doi: 10.1007/s00227-012-2057-8.

1020 Searcy-Bernal, R., Salas-Garza, A.E., Flores-Aguilar, R.A., Hinojosa-Rivera, P.R., 1992. Simultaneous
1021 comparison of methods for settlement and metamorphosis induction in the red abalone (*Haliotis*
1022 *rufescens*). *Aquaculture* 105, 241-250. doi: 10.1016/0044-8486(92)90090-8.

1023 Slattery, M., 1992. Larval settlement and juvenile survival in the red abalone (*Haliotis rufescens*), an
1024 examination of inductive cues and substrate selection. *Aquaculture* 102, 143-153. doi: 10.1016/0044-
1025 8486(92)90296-w.

1026 Tahil, A.S., Dy, D.T., 2016. Effects of reduced pH on the early larval development of hatchery-reared
1027 Donkey's ear abalone, *Haliotis asinina* (Linnaeus 1758). *Aquaculture* 459, 137-142. doi:
1028 10.1016/j.aquaculture.2016.03.027.

1029 Talmage, S.C., Gobler, C.J., 2011. Effects of elevated temperature and carbon dioxide on the growth and
1030 survival of larvae and juveniles of three species of northwest Atlantic bivalves. *PLoS One* 6, e26941-
1031 e26941. doi: 10.1371/journal.pone.0026941.

1032 Thiyagarajan, V., Ko, G.W.K., 2012. Larval growth response of the Portuguese oyster (*Crassostrea*
1033 *angulata*) to multiple climate change stressors. *Aquaculture* 370-371, 90-95. doi:
1034 10.1016/j.aquaculture.2012.09.025.

1035 Travers, M.-A., Basuyaux, O., Le Goïc, N., Huchette, S., Nicolas, J.-L., Koken, M., Paillard, C., 2009.
1036 Influence of temperature and spawning effort on *Haliotis tuberculata* mortalities caused by *Vibrio*
1037 *harveyi*: an example of emerging vibriosis linked to global warming. *Global Change Biol.* 15, 1365-
1038 1376. doi: 10.1111/j.1365-2486.2008.01764.x.

1039 Waldbusser, G.G., Hales, B., Langdon, C.J., Haley, B.A., Schrader, P., Brunner, E.L., Gray, M.W.,
1040 Miller, C.A., Gimenez, I., Hutchinson, G., 2015. Ocean acidification has multiple modes of action on
1041 bivalve larvae. *PLoS One* 10, e0128376-e0128376. doi: 10.1371/journal.pone.0128376.

1042 Wei, J., Carroll, R.J., Harden, K.K., Wu, G., 2012. Comparisons of treatment means when factors do not
1043 interact in two-factorial studies. *Amino Acids* 42, 2031-2035. doi: 10.1007/s00726-011-0924-0.

1044 Wessel, N., Martin, S., Badou, A., Dubois, P., Huchette, S., Julia, V., Nunes, F., Harney, E., Paillard, C.,
1045 Auzoux-Bordenave, S., 2018. Effect of CO₂-induced ocean acidification on the early development

1046 and shell mineralization of the European abalone (*Haliotis tuberculata*). J. Exp. Mar. Biol. Ecol. 508,
1047 52-63. doi: 10.1016/j.jembe.2018.08.005.

1048 Williams, E.A., Craigie, A., Yeates, A., Degnan, S.M., 2008. Articulated coralline algae of the genus
1049 amphiroa are highly effective natural inducers of settlement in the tropical abalone *Haliotis asinina*.
1050 The Biological Bulletin 215, 98-107. doi: 10.2307/25470687.

1051 Zippay, M.L., Hofmann, G.E., 2010. Effect of pH on gene expression and thermal tolerance of early life
1052 history stages of red abalone (*Haliotis rufescens*). J. Shellfish Res. 29, 429-439. doi:
1053 10.2983/035.029.0220.

1054 Gattuso, J.P., Magnan, A., Billé, R., Cheung, W.W., Howes, E.L., Joos, F., Allemand, D., Bopp, L.,
1055 Cooley, S.R., Eakin, C.M., Hoegh-Guldberg, O., 2015. Contrasting futures for ocean and society
1056 from different anthropogenic CO₂ emissions scenarios. Science, 349(6243). DOI:
1057 10.1126/science.aac4722.

1058 Gac, J.P., Marrec, P., Cariou, T., Guillerm, C., Macé, É., Vernet, M., Bozec, Y., 2020. Cardinal Buoys:
1059 An Opportunity for the Study of Air-Sea CO₂ Fluxes in Coastal Ecosystems. Front. Mar. Sci. 7, 712.

1060 Knights, A.M., Norton, M.J., Lemasson, A.J., Stephen, N., 2020. Ocean acidification mitigates the
1061 negative effects of increased sea temperatures on the biomineralization and crystalline ultrastructure
1062 of *Mytilus*. Front. Mar. Sci. 7, 773.

1063 García, E., Clemente, S., Hernández, J.C., 2015. Ocean warming ameliorates the negative effects of ocean
1064 acidification on *Paracentrotus lividus* larval development and settlement. Mar. Environ. Res. 110,
1065 61-68.

1066 Jiang, L., Zhang, F., Guo, M.L., Guo, Y.J., Zhang, Y.Y., Zhou, G.W., Cai, L., Lian, J.S., Qian, P.Y.,
1067 Huang, H., 2018. Increased temperature mitigates the effects of ocean acidification on the
1068 calcification of juvenile *Pocillopora damicornis*, but at a cost. Coral Reefs, 37, 71-79.

1069 Di Santo, V., 2015. Ocean acidification exacerbates the impacts of global warming on embryonic little
1070 skate, *Leucoraja erinacea* (Mitchill). J. Exp. Mar. Biol. Ecol. 463, 72-78.

1071 Kroeker, K.J., Gaylord, B., Hill, T.M., Hosfelt, J.D., Miller, S.H., Sanford, E., 2014. The role of
1072 temperature in determining species' vulnerability to ocean acidification: a case study using *Mytilus*
1073 *galloprovincialis*. PloS one, 9, p.e100353.

1074 Davis, A.R., Coleman, D., Broad, A., Byrne, M., Dworjanyn, S.A., Przeslawski, R., 2013. Complex
1075 responses of intertidal molluscan embryos to a warming and acidifying ocean in the presence of UV
1076 radiation. PloS one, 8, p.e55939.

1077 D'Amario, B., Pérez, C., Grelaud, M., Pitta, P., Krasakopoulou, E., Ziveri, P., 2020. Coccolithophore
1078 community response to ocean acidification and warming in the Eastern Mediterranean Sea: results
1079 from a mesocosm experiment. Scientific Reports, 10, 1-14.

1080 Zittier, Z.M.C., Bock, C., Sukhotin, A.A., Häfker, N.S., Pörtner, H.O., 2018. Impact of ocean
1081 acidification on thermal tolerance and acid–base regulation of *Mytilus edulis* from the White Sea.
1082 Polar Biol. 41, 2261-2273.

1083 Rodolfo-Metalpa, R., Houlbrèque, F., Tambutté, É., Boisson, F., Baggini, C., Patti, F.P., Jeffree, R., Fine,
1084 M., Foggo, A., Gattuso, J.P., Hall-Spencer, J.M., 2011. Coral and mollusc resistance to ocean
1085 acidification adversely affected by warming. Nat. Clim. Chang. 1, 308-312.

1086 Swezey, D.S., Boles, S.E., Aquilino, K.M., Stott, H.K., Bush, D., Whitehead, A., Rogers-Bennett, L.,
1087 Hill, T.M., Sanford, E., 2020. Evolved differences in energy metabolism and growth dictate the
1088 impacts of ocean acidification on abalone aquaculture. PNAS, 117, 26513-26519.

1089

1090

1091

1092

1093

1094